NODE IDENTIFIERS: COMPACT, DISCRETE REPRESENTATIONS FOR EFFICIENT GRAPH LEARNING

Yuankai Luo[1,2] **Hongkang Li**[3*] **Qijiong Liu**[2*] **Lei Shi**[1†] **Xiao-Ming Wu**[2†]

[1]Beihang University [2]The Hong Kong Polytechnic University [3]Rensselaer Polytechnic Institute

ABSTRACT

We present a novel end-to-end framework that generates highly compact (typically 6-15 dimensions), discrete (int4 type), and interpretable node representations—termed node identifiers (node IDs)—to tackle inference challenges on large-scale graphs. By employing vector quantization, we compress continuous node embeddings from multiple layers of a Graph Neural Network (GNN) into discrete codes, applicable under both self-supervised and supervised learning paradigms. These node IDs capture high-level abstractions of graph data and offer interpretability that traditional GNN embeddings lack. Extensive experiments on 34 datasets, encompassing node classification, graph classification, link prediction, and attributed graph clustering tasks, demonstrate that the generated node IDs significantly enhance speed and memory efficiency while achieving competitive performance compared to current state-of-the-art methods.

1 INTRODUCTION

Machine learning on graphs involves leveraging graph topology and node/edge attributes to perform various tasks, including node and graph classification (Hu et al., 2020; Luo et al., 2023b), link prediction (Lü & Zhou, 2011; Zhang & Chen, 2018), community detection (Fortunato, 2010; Fortunato & Hric, 2016), and recommendation (Konstas et al., 2009). Various methods have been developed to address these challenges, including random walk based-models (Perozzi et al., 2014; Grover & Leskovec, 2016), spectral methods (Bruna et al., 2013; Defferrard et al., 2016), and graph neural networks (GNNs) (Hamilton et al., 2017; Kipf & Welling, 2017; Veličković et al., 2018a). GNNs employ a message-passing mechanism (Gilmer et al., 2017) to iteratively aggregate information from a node's neighbors. This process enables GNNs to learn node representations by effectively integrating graph topology and node attributes, leading to impressive results across various tasks.

Despite the advancements in GNNs, their application to large-scale scenarios requiring low latency and fast inference remains challenging (Zhang et al., 2020; Jia et al., 2020; Yang et al., 2024). The inherent bottleneck is the message-passing mechanism, which necessitates loading the entire graph—potentially comprising billions of edges—during inference for target nodes, which is computationally demanding and time-consuming. To address this challenge, recent studies (Zhang et al., 2021b; Tian et al., 2022; Yang et al., 2024) have explored knowledge distillation techniques to distill a small MLP model that captures essential information from a pre-trained GNN, making it suitable for latency-critical applications (Tian et al., 2023). However, these GNN-to-MLP methods require supervised training using class labels and lack the ability to generate effective node representations.

An alternative approach to facilitate inference on large-scale graphs involves learning effective, low-dimensional node embeddings that can be directly utilized for downstream prediction tasks. This method has been extensively explored in early works on network/graph embedding, such as DeepWalk (Perozzi et al., 2014) and node2vec (Grover & Leskovec, 2016), as well as in recent efforts leveraging GNNs to learn embeddings for graph tokens (Liu et al., 2024d;a; Qu et al., 2024; Xia et al., 2023), including nodes, edges, and (sub)graphs. To balance representation effectiveness and computational efficiency, embeddings generated by GNNs typically have dimensions of 128 or 256. However, this

---

*Contributed equally as the second authors.

†Corresponding authors. Correspondence to: luoyk@buaa.edu.cn, xiao-ming.wu@polyu.edu.hk.
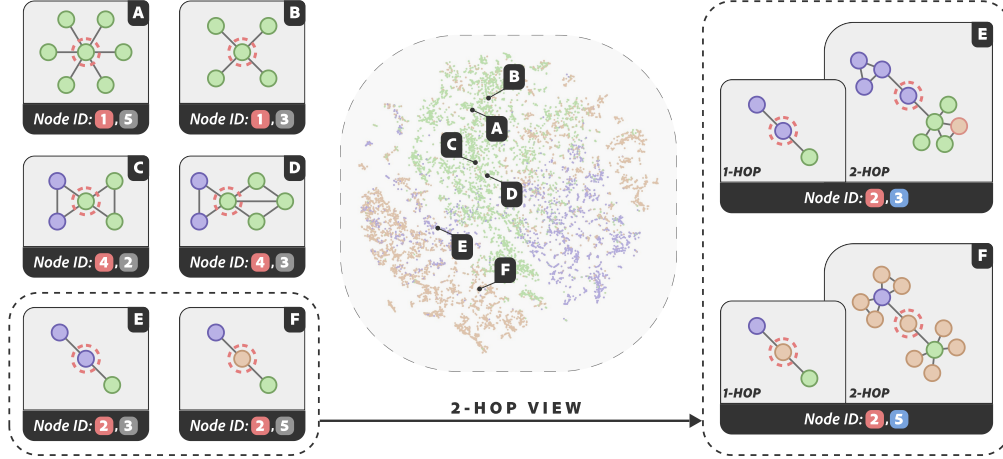
Figure 1: Illustration of 2-dimensional node IDs generated by our NID framework using a two-layer GCN. The first ID code is derived from the first-layer node embeddings, and the second ID code from the second-layer embeddings. *Center:* t-SNE visualization of node embeddings in the PubMed Dataset, with colors indicating different class labels. *Left:* Six nodes are shown with their IDs and 1-hop neighborhoods (topology and label distribution). Nodes sharing the same first ID code have similar 1-hop neighborhoods, though not necessarily the same class label. *Right:* Nodes E and F are further analyzed with their 2-hop neighborhoods, where differences are reflected in their distinct second ID code (blue) and class label.

relatively high dimensionality poses challenges in terms of storage and computational efficiency for large-scale applications. Furthermore, the real-valued embeddings often lack interpretability.

In this work, we tackle this challenge by learning highly compact (typically 6-15 dimensions), discrete (int4 type), and interpretable node representations, termed node identifiers (node IDs). We introduce a novel end-to-end framework called NID, which employs vector quantization (Gray, 1984) to compress the continuous node embeddings generated at each layer of a GNN into discrete codes, where the GNN and codebooks are trained jointly. This approach effectively captures the multi-order neighborhood structures within the graph. Fig. 1 illustrates examples of two-dimensional node IDs generated by a two-layer GNN, demonstrating their ability to capture multi-level structural patterns, as well as their interpretability. We summarize the significance of our work as follows:

- We empirically and theoretically demonstrate the feasibility of learning highly compact, discrete codes (node IDs) as effective node representations for efficient graph learning, without relying on knowledge distillation. Our extensive evaluation across 34 diverse datasets and tasks—including node and graph classification, link prediction, and attributed graph clustering—shows that these node IDs achieve performance competitive with state-of-the-art methods while significantly enhancing speed and memory efficiency. We also offer a theoretical justification for our approach.

- Our proposed NID framework can be integrated with state-of-the-art unsupervised and supervised GNN methods to enhance performance. Experiments demonstrate that the generated node IDs not only retain essential information from GNN embeddings but also uncover hidden patterns in some cases, leading to significantly improved performance. This warrants deeper investigation.

- Our findings indicate significant redundancy in GNN embeddings. The generated compact, discrete node IDs provide a high-level abstraction of graph data, offering interpretability that GNN embeddings lack. This may facilitate graph tokenization and applications involving LLMs.

2 PRELIMINARIES

We define a graph as a tuple $\mathcal{G} = (\mathcal{V}, \mathcal{E}, \boldsymbol{X})$, where $\mathcal{V}$ is the set of nodes, $\mathcal{E} \subseteq \mathcal{V} \times \mathcal{V}$ is the set of edges, and $\boldsymbol{X} \in \mathbb{R}^{|\mathcal{V}| \times d}$ is the node feature matrix, with $|\mathcal{V}|$ representing the number of nodes and d the dimension of the node features. Let $\boldsymbol{A} \in \mathbb{R}^{|\mathcal{V}| \times |\mathcal{V}|}$ denote the adjacency matrix of $\mathcal{G}$.

Message Passing Neural Networks (MPNNs) have become the dominant approach for learning graph representations. A typical example is graph convolutional networks (GCNs) (Kipf & Welling, 2017). Gilmer et al. (2017) reformulated early GNNs into a framework of message passing GNNs, which computes representations $\boldsymbol{h}_v^l$ for any node v in each layer l as:

$$\boldsymbol{h}_v^l = \text{UPDATE}^l \left(\boldsymbol{h}_v^{l-1}, \text{AGG}^l \left(\left\{ \boldsymbol{h}_u^{l-1} \mid u \in \mathcal{N}(v) \right\} \right) \right), \tag{1}$$

where $\mathcal{N}(v)$ denotes the neighborhood of v, AGG^l is the message function, and UPDATE^l is the update function. The initial node representation $\boldsymbol{h}_v^0$ is the node feature vector $\boldsymbol{x}_v \in \mathbb{R}^d$. The message function aggregates information from the neighbors of v to update its representation. The output of the last layer, i.e., $\mathrm{MPNN}(v, \boldsymbol{A}, \boldsymbol{X}) = \boldsymbol{h}_v^L$, is the representation of v produced by the MPNN.

Prediction tasks on graphs involve node-level, edge-level, and graph-level tasks. Each type of tasks requires a tailored graph readout function, R, which aggregates the output node representations, $\boldsymbol{h}_v^L$, from the last layer L, to compute the final prediction result:

$$\boldsymbol{h}_{\text{readout}} = \mathrm{R}\left(\left\{\boldsymbol{h}_v^L, v \in \mathcal{V}\right\}\right). \tag{2}$$

Specifically, for *node-level* tasks, which involve classifying individual nodes, R is simply an identity mapping. For *edge-level* tasks, which focus on analyzing the relationship between any node pair (u, v), R is typically modeled as the Hadamard product of the node representations (Kipf & Welling, 2016), i.e., $\boldsymbol{h}_{\text{readout}} = \boldsymbol{h}_v^L \odot \boldsymbol{h}_u^L$. For *graph-level* tasks that aim to make predictions about the entire graph, R often functions as a global mean pooling operation, expressed as $\boldsymbol{h}_{\text{readout}} = \frac{1}{|\mathcal{V}|} \sum_{v \in \mathcal{V}} \boldsymbol{h}_v^L$.

Vector Quantization (VQ) (Gray, 1984) aims to represent a large set of vectors, $\boldsymbol{Z} = \{\boldsymbol{z}_i\}_{i=1}^N$, with a small set of prototype (code) vectors of a codebook $\boldsymbol{C} = \{\boldsymbol{e}_k\}_{k=1}^K$, where $N \gg K$. The codebook is often created using algorithms such as k-means clustering via optimizing the following objective:

$$\textbf{VQ:} \quad \min_{\boldsymbol{C}} \sum_{i=1}^N \min_{k=1}^K ||\boldsymbol{z}_i - \boldsymbol{e}_k||_2^2. \tag{3}$$

Once the codebook is learned, each vector $\boldsymbol{z}_i$ can be approximated by its closet prototype vector $\boldsymbol{e}_t$, where $t = \arg\min_k ||\boldsymbol{z}_i - \boldsymbol{e}_k||_2^2$ is the index of the prototype vector. **Residual Vector Quantization (RVQ)** (Juang & Gray, 1982; Martinez et al., 2014) extends the basic VQ by performing the quantization process M times. Initially, a standard VQ is performed. Then, the *residual vector* is calculated:

$$\boldsymbol{r}_i = \boldsymbol{z}_i - \boldsymbol{e}_t, \tag{4}$$

which represents the quantization error from the initial quantization. Then, the residual vectors $\boldsymbol{r}_i$ are quantized using a second codebook. This process can be performed repeatedly, with each stage quantizing the residual error from the previous stage, ultimately producing M tiers of codes.

3 OUR PROPOSED NODE ID (NID) FRAMEWORK

Our proposed NID framework consists of two stages:

1. *Generating compact, discrete node IDs.* Nodes are encoded using multi-layer MPNNs to capture multi-order neighborhood structures. At each layer, the node embedding is quantized into a tuple of structural codewords. The tuples are then combined to form what we refer to as the node ID.

2. *Utilizing the generated node IDs as node representations in various downstream tasks.* We directly use the node IDs for unsupervised tasks such as node clustering. We train simple MLPs with the node IDs for supervised tasks including node classification, link prediction, and graph classification.

3.1 GENERATION OF NODE IDS

Fig. 2 illustrates the diverse clustering patterns of node representations produced by an MPNN at different layers l. This diversity arises from the cumulative smoothing effect caused by successive applications of graph convolution at each layer (Li et al., 2018; 2019). To generate structure-aware node IDs, we employ an L-layer MPNN to capture multi-order neighborhood structures. At each layer, we use vector quantization to encode the node embeddings produced by the MPNN into
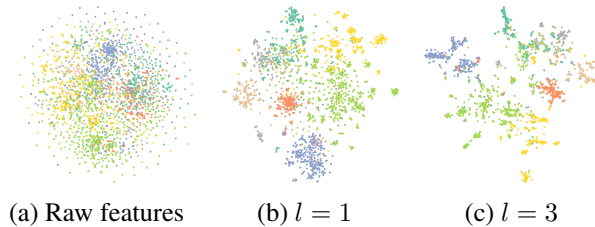

(a) Raw features   (b) $l = 1$ (c) $l = 3$

Figure 2: t-SNE visualization of the node representations of the Cora dataset generated by an MPNN at different layers l.
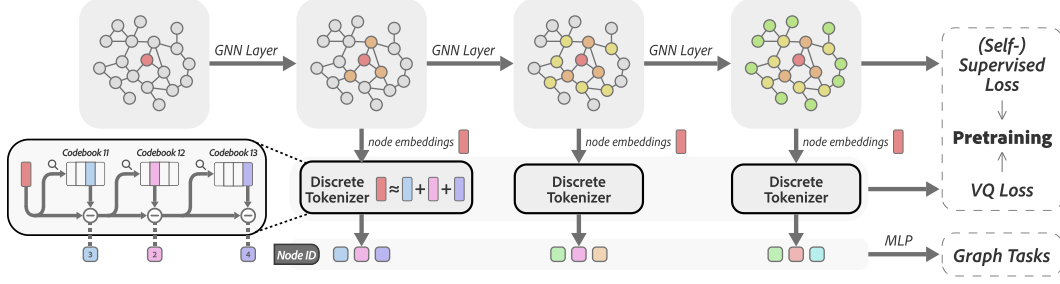
Figure 3: Overview of our proposed NID framework.

M codewords (integer indices). For each node v, we define the node ID of v as a tuple composed of $L \times M$ codewords, structured as follows:

$$\text{Node\_ID}(v) = (c_{11}, \cdots, c_{1M}, c_{21}, \cdots, c_{2M}, \cdots, c_{L1}, \cdots, c_{LM}), \tag{5}$$

where c_{lm} represents the m-th codeword at the l-th layer. Both M and L can be very small. For the node IDs in Fig. 1, $M = 1$ and $L = 2$. In our experiments, we typically set $M = 3$ and $L \in [2, 5]$.

Learning Node IDs. As illustrated in Fig. 3, at each layer l ($1 \le l \le L$) of the MPNN, we employ RVQ to quantize the node embeddings and produce M tiers of codewords for each node v (see App. E.1 for a detailed explanation). Each codeword c_{lm} ($1 \le m \le M$) is generated by a *distinct* codebook $\boldsymbol{C}_{lm} = \{\boldsymbol{e}_k^{lm}\}_{k=1}^K$, where K is the size of the codebook. Hence, there are a total of $L \times M$ codebooks, indexed by lm. Let $\boldsymbol{r}_{lm}$ denote the vector to be quantized. Note that $\boldsymbol{r}_{l1}$ is the node embedding $\boldsymbol{h}_v^l$ produced by the MPNN. When $m > 1$, $\boldsymbol{r}_{lm}$ represents the residual vector. Then, $\boldsymbol{r}_{lm}$ is approximated by its nearest code vector from the corresponding codebook $\boldsymbol{C}_{lm}$:

$$c_{lm} = \arg\min_k ||\boldsymbol{r}_{lm} - \boldsymbol{e}_k^{lm}||, \tag{6}$$

producing the codeword c_{lm}, which is the index of the nearest code vector.

We introduce a simple, generic framework for learning node IDs (codewords c_{lm}) by jointly training the MPNN and the codebooks with the following loss function:

$$\mathcal{L}_{\text{NID}} = \mathcal{L}_{\mathcal{G}} + \mathcal{L}_{\text{VQ}}, \tag{7}$$

where $\mathcal{L}_{\mathcal{G}}$ is a (self-)supervised graph learning objective, and $\mathcal{L}_{\text{VQ}}$ is a vector quantization loss. $\mathcal{L}_{\mathcal{G}}$ aims to train the MPNN to produce effective node embeddings, while $\mathcal{L}_{\text{VQ}}$ ensures the codebook vectors align well with the node embeddings. For a single node v, $\mathcal{L}_{\text{VQ}}$ is defined as

$$\mathcal{L}_{\text{VQ}} = \sum_{l=1}^{L} \sum_{m=1}^{M} ||\text{sg}(\boldsymbol{r}_{lm}) - \boldsymbol{e}_{c_{lm}}^{lm}|| + \beta ||\boldsymbol{r}_{lm} - \text{sg}(\boldsymbol{e}_{c_{lm}}^{lm})||, \tag{8}$$

where sg denotes the stop gradient operation, and β is a weight parameter. The first term in Eq. (8) is the *codebook loss* (Van Den Oord et al., 2017), which only affects the codebook and brings the selected code vector close to the node embedding. The second term is the *commitment loss* (Van Den Oord et al., 2017), which only influences the node embedding and ensures the proximity of the node embedding to the selected code vector. In practice, we can use exponential moving averages (Razavi et al., 2019) as a substitute for the *codebook loss*.

Self-supervised Learning. The graph learning objective $\mathcal{L}_{\mathcal{G}}$ can be a self-supervised learning task, such as graph reconstruction (i.e., reconstructing the node features or adjacency matrix) or contrastive learning (Liu et al., 2021). In this paper, we examine two representative models: GraphMAE (Hou et al., 2022) and GraphCL (You et al., 2020). We discuss GraphMAE here and address GraphCL in the App. A due to space limitations. Specifically, GraphMAE involves sampling a subset of nodes $\tilde{\mathcal{V}} \subset \mathcal{V}$, masking the node features as $\tilde{\boldsymbol{X}}$, encoding the masked node features using an MPNN, and subsequently reconstructing the masked features with a decoder. The reconstruction loss is based on the scaled cosine error, expressed as:

$$\mathcal{L}_{\mathcal{G}} = \mathcal{L}_{\text{MAE}} = \frac{1}{|\tilde{\mathcal{V}}|} \sum_{v \in \tilde{\mathcal{V}}} \left(1 - \frac{\boldsymbol{x}_v^T \boldsymbol{z}_v}{||\boldsymbol{x}_v|| \cdot ||\boldsymbol{z}_v||} \cdot \gamma \right),$$

where $\tilde{\mathcal{V}}$ is the set of masked nodes, $\boldsymbol{z}_v = f_D(\tilde{\boldsymbol{h}}_v^L)$ is the reconstructed node features by a decoder f_D, $\tilde{\boldsymbol{h}}_v^L = \text{MPNN}(v, \boldsymbol{A}, \tilde{\boldsymbol{X}})$, and $\gamma \ge 1$ is a scaling factor. Let $\tilde{\boldsymbol{r}}_{l1} := \tilde{\boldsymbol{h}}_v^l$ denote the node embedding generated by the l-th layer of the MPNN with the masked features. The overall training loss is

$$\mathcal{L}_{\text{NID}} = \mathcal{L}_{\text{MAE}} + \sum_{v \in \tilde{\mathcal{V}}} \sum_{l=1}^{L} \sum_{m=1}^{M} \|\text{sg}(\tilde{\boldsymbol{r}}_{lm}) - \boldsymbol{e}_{c_{lm}}\| + \beta \|\tilde{\boldsymbol{r}}_{lm} - \text{sg}(\boldsymbol{e}_{c_{lm}})\|. \tag{9}$$

Supervised Learning. The graph learning objective $\mathcal{L}_{\mathcal{G}}$ can also be a supervised learning task, such as node classification, link prediction, or graph classification. For classification tasks, $\mathcal{L}_{\mathcal{G}}$ can be the cross-entropy loss between the target label y and the prediction $\boldsymbol{h}_{\text{readout}}$ (see Eq. (2)):

$$\mathcal{L}_{\mathcal{G}} = \mathcal{L}_{\text{CE}}(y, \boldsymbol{h}_{\text{readout}}). \tag{10}$$

Remark. Our NID framework differs from VQ-VAE (Van Den Oord et al., 2017) and similar approaches (Lee et al., 2022; Yang et al., 2024) in codebook learning. Unlike these methods, our training objective $\mathcal{L}_{\text{NID}}$ does not involve using the code vectors ($\boldsymbol{e}_k$) for a reconstruction task. Instead, we guide the codebook learning process solely via graph learning tasks ($\mathcal{L}_{\mathcal{G}}$). This is because our experiments show that omitting the reconstruction loss has a negligible impact on performance (see Appendix D.5 for details). Moreover, our NID framework is compatible with any MPNN model. In experiments, we use popular models like GCN (Kipf & Welling, 2017), GAT (Veličković et al., 2018a), SAGE (Hamilton et al., 2017) and GIN (Xu et al., 2018).

3.2 Applications of Node IDs for Graph Learning

The generated node IDs can be considered as highly compact node representations and used directly for various downstream graph learning tasks, as outlined below.

Node-level tasks include *node classification* and *node clustering*. For node classification, each node v in the graph is associated with a label y_v, representing its category. We can directly utilize the node IDs of the labeled nodes to train an MLP network for classification. The prediction is formulated as

$$\hat{y}_v = \text{MLP}(\text{Node\_ID}(v)). \tag{11}$$

For node clustering, one can directly apply vector-based clustering algorithms such as k-means (Mac-Queen et al., 1967) to the node IDs to obtain clustering results.

Edge-level tasks typically involve *link prediction*. The aim is to predict whether an edge should exist between any node pair (u, v). The prediction can be made by

$$\hat{y}_{(u,v)} = \text{MLP}(\text{Node\_ID}(u) \odot \text{Node\_ID}(v)), \tag{12}$$

where $\odot$ is the Hadamard product.

Graph-level tasks include *graph classification* and *graph regression*. These tasks involve predicting a categorical label or numerical value for the entire graph $\mathcal{G}$. The prediction can be formulated as

$$\hat{y}_{\mathcal{G}} = \text{MLP}\left(\frac{1}{|\mathcal{V}|} \sum_{v \in \mathcal{V}} \text{Node\_ID}(v)\right), \tag{13}$$

where a global mean pooling function is applied on all the node IDs to generate a representation for the graph $\mathcal{G}$, which is then input into an MLP for prediction. Note that the selection of the readout function, such as mean pooling, is considered a hyper-parameter.

Remark. Due to the high compactness of the node IDs, which usually consists of multiple codewords (int4 type in our experiments), the inference process of the aforementioned graph learning tasks can be *greatly accelerated*. Furthermore, as illustrated in Fig. 1, the node IDs represent a high-level abstraction of structure-aware information in a graph, enabling them to achieve competitive performance across various tasks, as evidenced in our evaluation.

3.3 Theoretical Analysis

We provide a theoretical analysis to verify the validity of the proposed method with a simplified model. We prove the optimized codebook by VQ can distinguish nodes based on a widely used data formulation, which leads to a desired classification performance by training a linear layer.

Theoretical formulation. Consider a node-level P-classification problem on a graph $\mathcal{G} = \{\mathcal{V}, \mathcal{E}, \boldsymbol{X}\}$ with $\boldsymbol{A} \in \mathbb{R}^{|\mathcal{V}| \times |\mathcal{V}|}$ as the adjacency matrix and $\boldsymbol{Y}$ as the labels. We use a one-layer GCN to generate

Table 1: Node classification results in supervised representation learning over homophilic and heterophilic graphs (%). The baseline results are primarily taken from Polynormer (Deng et al., 2024).

Transductive	Cora	CiteSeer	PubMed	Computer	Photo	CS	Physics	WikiCS	Squirrel	Chameleon	Ratings	Questions
# nodes	2,708	3,327	19,717	13,752	7,650	18,333	34,493	11,701	2223	890	24,492	48,921
# edges	5,278	4,732	44,324	245,861	119,081	81,894	247,962	216,123	46,998	8,854	32,927	153,540
Metric	Accuracy↑	Accuracy↑	Accuracy↑	Accuracy↑	Accuracy↑	Accuracy↑	Accuracy↑	Accuracy↑	Accuracy↑	Accuracy↑	Accuracy↑	ROC-AUC↑
GPRGNN	87.95 $\pm$1.18	77.13 $\pm$1.67	87.54 $\pm$0.38	89.32 $\pm$0.29	94.49 $\pm$0.14	95.13 $\pm$0.09	96.85 $\pm$0.08	78.12 $\pm$0.23	38.95 $\pm$1.99	39.93 $\pm$3.30	44.88 $\pm$0.34	55.48 $\pm$0.91
APPNP	87.87 $\pm$0.82	76.53 $\pm$1.16	88.43 $\pm$0.15	90.18 $\pm$0.17	94.32 $\pm$0.14	94.49 $\pm$0.07	96.54 $\pm$0.07	78.87 $\pm$0.11	36.88 $\pm$1.27	41.62 $\pm$3.13	52.74 $\pm$0.73	77.82 $\pm$1.31
SGFormer	87.83 $\pm$0.92	77.24 $\pm$0.74	89.31 $\pm$0.54	92.42 $\pm$0.66	95.58 $\pm$0.36	95.71 $\pm$0.24	96.75 $\pm$0.26	80.05 $\pm$0.46	42.65 $\pm$2.41	45.21 $\pm$3.72	54.14 $\pm$0.62	73.81 $\pm$0.59
Polynormer	88.11 $\pm$1.08	76.77 $\pm$1.01	87.34 $\pm$0.43	93.18 $\pm$0.18	96.11 $\pm$0.23	95.51 $\pm$0.29	97.22 $\pm$0.06	79.53 $\pm$0.83	40.87 $\pm$1.96	41.82 $\pm$3.45	54.46 $\pm$0.40	78.92 $\pm$0.89
Graph-MLP	87.06 $\pm$1.38	76.43 $\pm$1.44	88.93 $\pm$0.63	90.78 $\pm$0.41	95.43 $\pm$0.76	94.68 $\pm$0.28	95.45 $\pm$0.24	75.35 $\pm$0.55	-	-	-	-
VQGraph	86.11 $\pm$1.26	75.64 $\pm$0.92	88.03 $\pm$0.63	90.28 $\pm$0.47	94.98 $\pm$0.59	93.82 $\pm$0.17	95.93 $\pm$0.28	77.92 $\pm$0.61	-	-	-	-
GCN	88.77 $\pm$0.61	77.53 $\pm$0.92	90.04 $\pm$0.25	93.78 $\pm$0.31	96.14 $\pm$0.21	95.94 $\pm$0.28	97.36 $\pm$0.07	80.91 $\pm$0.81	44.50 $\pm$1.92	46.11 $\pm$3.16	53.57 $\pm$0.32	77.40 $\pm$1.07
NID$_{\text{GCN}}$	87.88 $\pm$0.69	76.89 $\pm$1.09	89.42 $\pm$0.44	93.41 $\pm$0.08	96.17 $\pm$0.04	95.52 $\pm$0.10	97.34 $\pm$0.04	78.55 $\pm$0.15	**45.09** $\pm$1.72	**46.29** $\pm$2.92	53.55 $\pm$0.13	96.85 $\pm$0.10
GAT	88.22 $\pm$1.24	77.08 $\pm$0.84	89.47 $\pm$0.25	93.53 $\pm$0.18	96.27 $\pm$0.15	94.46 $\pm$0.14	97.17 $\pm$0.09	80.98 $\pm$0.83	38.72 $\pm$1.46	43.44 $\pm$3.00	54.88 $\pm$0.74	78.35 $\pm$1.16
NID$_{\text{GAT}}$	87.35 $\pm$0.57	76.13 $\pm$1.35	88.97 $\pm$0.36	93.38 $\pm$0.16	**96.47** $\pm$0.27	94.75 $\pm$0.16	97.13 $\pm$0.08	79.56 $\pm$0.43	37.68 $\pm$2.04	42.83 $\pm$3.42	**54.92** $\pm$0.42	**97.03** $\pm$0.02

the node embedding $\boldsymbol{h}_v$ for $v \in \mathcal{V}$, i.e., $\boldsymbol{h}_v = \sigma\left(\frac{1}{|\mathcal{N}(u)|} \sum_{u \in \mathcal{N}(u)} \boldsymbol{W} \boldsymbol{x}_u\right)$, where $\boldsymbol{W} \in \mathbb{R}^{d' \times d}$ and we assume $\sigma(\cdot)$ as an identity function. Given the obtained natural number Node_ID$(v) \in \mathbb{N}^r$ for node $v \in \mathcal{V}$, $r < K$, we map each entry to a d_e-dimensional embedding, where different digits correspond to orthogonal embeddings. Hence, Node_ID(v) is projected to a rd_e-dimensional vector, denoted by $\boldsymbol{z}_v$. We use nodes from $\mathcal{V}_R$ to train a linear head $\boldsymbol{V} \in \mathbb{R}^{rd_e \times P}$, i.e., $\min_{\boldsymbol{V}} \frac{1}{|\mathcal{V}_R|} \sum_{v \in \mathcal{V}_R} \ell(\boldsymbol{z}_v, y_v; \boldsymbol{V})$, where $\ell(\boldsymbol{z}_v, y_v; \boldsymbol{V}) = -\boldsymbol{y}_i^\top \log(\hat{\boldsymbol{p}}_v) := -\boldsymbol{y}_i^\top \log(\mathrm{softmax}(\boldsymbol{z}_v^\top \boldsymbol{V}))$. Here $\boldsymbol{y}_i$ is the one-hot vector of $y_i \in \mathbb{N}$, where only the $y_i + 1$-th entry is 1 and others are 0. The classification error is defined by $\mathbb{1}[y_v \neq \arg\max_{i \in [P]} \hat{\boldsymbol{p}}_{v,i}]$ for $v \in \mathcal{V}$, where $\hat{\boldsymbol{p}}_{v,i}$ is the i-th entry of $\hat{\boldsymbol{p}}_v$.

We define a set of orthonormal vectors $\{\boldsymbol{\mu}_i\}_{i=1}^Q$. For a P-classification problem ($P < Q$), denote $\{\boldsymbol{\mu}_i\}_{i=1}^P$ as the set of discriminative patterns that directly determine the label, while $\{\boldsymbol{\mu}_i\}_{i=P+1}^Q$ as the set of non-discriminative patterns that are irrelevant to the label. Specifically, we assume that for any node $v \in \mathcal{V}$ with label $p \in [P]$, $\boldsymbol{x}_v = \boldsymbol{\mu}_p$ or at least one of its neighbor equals $\boldsymbol{\mu}_p$, and no neighbor of $\boldsymbol{x}_v$ or itself equals $\boldsymbol{\mu}_j$ for $j \in [P], j \neq p$. This formulation extends from binary node classification in (Zhang et al., 2023b; Li et al., 2024), which is verified on real-world datasets. We also assume rows of the optimized $\boldsymbol{W}$ by (7) are in directions of $\boldsymbol{\mu}_i, i \in [P]$ uniformly by theoretical findings in (Zhang et al., 2023b; Li et al., 2024). Then, we have the following theorem.

Theorem 1. *The optimizer $\boldsymbol{C}^*$ of VQ objective (7) satisfies that, for any $\boldsymbol{x}_u$ and $\boldsymbol{x}_v$, $u, v \in \mathcal{V}$ with different labels, Node_ID$(u) \neq$ Node_ID(v). Then, as long as $\mathcal{V}_R$ uniformly include node IDs from all the classes, by training the linear head $\boldsymbol{V}$ with sufficient gradient descent steps, we can achieve that the classification error $\mathbb{1}[y_v \neq \arg\max_{i \in [P]} \hat{\boldsymbol{p}}_{v,i}] = 0$ for any $v \in \mathcal{V}$.*

Remark. Theorem 1 illustrates that the optimized $\boldsymbol{C}^*$ of VQ objective (7) ensures that the obtained IDs from different classes are distinct. Then, we demonstrate that with node IDs in the training set, a linear head can be learned to achieve a zero classification error. The proof can be found in App. B.

4 EVALUATION

In this section, we demonstrate the versatility of our NID framework across various graph learning tasks. We detail its application in two distinct scenarios:

- **Supervised representation learning for node classification, link prediction and graph classification.** Here, we evaluate our NID against several SOTA models for graph representation learning, following learning protocols (Luo et al., 2024b; Rampášek et al., 2022; Wang et al., 2023c).
- **Unsupervised representation learning for attributed graph clustering, node classification, and graph classification.** In these unsupervised tasks, NID is benchmarked against well-known contrastive and generative SSL methods. We adhere strictly to the established experimental procedures as the standard settings (Bhowmick et al., 2024; Hou et al., 2022; You et al., 2020).

Detailed datasets, baselines, and hyperparameters are provided in App. C due to space constraints.

4.1 OVERALL PERFORMANCE

The learned node IDs, **typically comprising 6 to 15 int4 integers**, serve as effective node representations. They achieve competitive or superior performance across a wide range of tasks while significantly enhancing speed and memory efficiency. Additionally, our NID framework can be integrated with SOTA supervised or unsupervised GNN methods to enhance performance.

Table 2: Node classification results in supervised representation learning on large-scale graphs (%).

Transductive	ogbn-proteins	ogbn-arxiv	ogbn-products	pokec
# nodes	132,534	169,343	2,449,029	1,632,803
# edges	39,561,252	1,166,243	61,859,140	30,622,564
Metric	ROC-AUC↑	Accuracy↑	Accuracy↑	Accuracy↑
GPRGNN	75.68 ±0.49	71.10 ±0.12	79.76 ±0.59	78.83 ±0.05
LINKX	71.37 ±0.58	66.18 ±0.33	71.59 ±0.71	82.04 ±0.07
GraphGPS	76.83 ±0.26	70.97 ±0.41	OOM	OOM
SGFormer	79.53 ±0.38	72.63 ±0.13	74.16 ±0.31	73.76 ±0.24
Polynormer	75.97 ±0.47	71.82 ±0.23	82.97 ±0.28	85.95 ±0.07
SAGE	79.43 ±0.75	72.67 ±0.31	83.27 ±0.35	85.97 ±0.21
Infer. Time	158.1ms	416.5ms	11.9s	129.6s
Storage Space	129.4MB	165.7MB	1.9GB	1.6GB
NID$_{SAGE}$	76.78 ±0.59	70.52 ±0.14	81.83 ±0.26	85.63 ±0.31
Infer. Time	0.4ms	0.3ms	0.7ms	27.1ms
Storage Space	0.4MB	1.2MB	17.5MB	16.4MB

Table 3: Graph-level performance in supervised representation learning from LRGB.

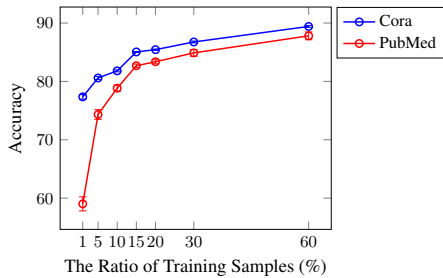| Inductive	Peptides-func	Peptides-struct
Avg. # nodes	150.9	150.9
Avg. # edges	307.3	307.3
Metric	AP↑	MAE↓
GT	0.6326 ±0.0126	0.2529 ±0.0016
GraphGPS	0.6535 ±0.0041	0.2500 ±0.0012
GRIT	0.6988 ±0.0082	0.2460 ±0.0012
Exphormer	0.6527 ±0.0043	0.2481 ±0.0007
Graph ViT	0.6970 ±0.0080	0.2449 ±0.0016
GCN	0.6762 ±0.0053	0.2512 ±0.0007
Infer. Time	471.1ms	424.9ms
NID$_{GCN}$	0.6608 ±0.0058	0.2589 ±0.0014
Infer. Time	0.4ms	0.4ms

Figure 4: Supervised node classification results of **NID**$_{GCN}$ with varying ratios of training samples.

Table 4: Link prediction in supervised representation learning. The baselines are from Wang et al. (2023c) (%).

Inductive	Cora	CiteSeer	PubMed	ogbl-collab
# nodes	2,708	3,327	19,717	235,868
# edges	5,278	4,552	44,324	1,285,465
Metric	HR@100↑	HR@100↑	HR@100↑	HR@50↑
SEAL	81.71 ±1.30	83.89 ±2.15	75.54 ±1.32	64.74 ±0.43
NBFnet	71.65 ±2.27	74.07 ±1.75	58.73 ±1.99	OOM
Neo-GNN	80.42 ±1.31	84.67 ±2.16	73.93 ±1.19	57.52 ±0.37
BUDDY	88.00 ±0.44	92.93 ±0.27	74.10 ±0.78	65.94 ±0.58
NCN	89.05 ±0.96	91.56 ±1.43	79.05 ±1.16	64.76 ±0.87
GCN	85.73 ±1.13	89.67 ±0.81	80.36 ±0.58	64.05 ±0.63
Inference Time	44.2ms	51.5ms	102.7ms	517.1ms
NID$_{GCN}$	**90.33** ±0.76	88.56 ±0.72	75.67 ±0.63	64.31 ±0.48
Inference Time	10.9ms	9.1ms	22.1ms	119.7ms

4.1.1 SUPERVISED NODE IDS FOR SUPERVISED REPRESENTATION LEARNING

Node Classification, Tables 1, 2, Figure 4. We have conducted extensive evaluations on 8 homophilic and 4 heterophilic graphs, testing scalability on 4 large-scale graphs, each with millions of nodes. Recently, Luo et al. (2024b; 2025b) observed that classic GNNs can achieve competitive performance in node classification with proper hyperparameter tuning. Building on this, we implement our NID on GCN, GAT and SAGE, maintaining all experimental settings as described by Luo et al. (2024b), as they match the hyperparameter search space used in SOTA Polynormer (Deng et al., 2024). We compare NID against SOTA GNNs and Graph Transformers (GTs). Additionally, we compare NID against SOTA GNN-to-MLP methods VQGraph and Graph-MLP under the same settings.

As demonstrated in Table 1, our NID performs competitively with SOTA methods on both homophilic and heterophilic graphs, suggesting that our compact discrete node IDs retain nearly all essential information compared to original GNN node embeddings. Furthermore, the performance comparison clearly shows the superior quality of our NID over SOTA GNN-to-MLP method VQGraph. Notably, NID surpasses all baselines across 4 heterophilic graphs. In a detailed analysis of Questions, we observe that **NID**$_{GCN}$ outperforms GCN by 20%. This dataset represents a highly imbalanced binary classification task, with 98% of nodes classified into the same category. This example illustrates that the node IDs may preserve information beyond that of original GNN node embeddings.

As shown in Table 2, **NID**$_{SAGE}$ not only achieves near-SOTA performance on datasets with millions of nodes but also maintains fast inference times; notably, **NID**$_{SAGE}$ achieves a speed increase ranging from 400× to 17,000× faster than SAGE across 4 large graphs. Remarkably, our IDs require only a small fraction of labels for training. For instance, in the case of the ogbn-products dataset, only 8% of the data is used for training. We analyze the training ratio in Figure 4, showing that merely 15% of the training dataset is sufficient to train node IDs that achieve effective predictive performance.

Graph Classification, Table 3. We compare NID against SOTA GNNs and GTs designed for graph-level tasks on two peptide graph benchmarks from LRGB (Dwivedi et al., 2022): Peptides-func and Peptides-struct. We take all evaluation protocols suggested by Rampášek et al. (2022). As evidenced in Table 3, applying pooling to the node IDs achieves excellent performance with notable efficiency improvement, highlighting the potential of NID for supervised learning in graph-level tasks.

Table 5: Attributed graph clustering results; normalized mutual information, and F1-score (%).

	Cora NMI↑	Cora F1↑	CiteSeer NMI↑	CiteSeer F1↑	PubMed NMI↑	PubMed F1↑	Computer NMI↑	Computer F1↑	Photo NMI↑	Photo F1↑	Physics NMI↑	Physics F1↑	ogbn-arxiv NMI↑	ogbn-arxiv F1↑
SBM	36.2	30.2	15.3	19.1	16.4	16.7	48.4	34.6	59.3	47.4	45.4	30.4	31.9	28.3
AGC	34.1	28.9	25.5	27.5	18.2	18.4	51.3	35.3	59.0	44.2	-	-	-	-
SDCN	27.9	29.9	31.4	41.9	19.5	29.9	24.9	45.2	41.7	45.1	50.4	39.9	15.3	28.8
DAEGC	8.3	13.6	4.3	18.0	4.4	11.6	42.5	37.3	47.6	45.0	-	-	-	-
NOCD	46.3	36.7	20.0	24.1	25.5	20.8	44.8	37.8	62.3	60.2	51.9	28.7	20.7	38.2
DiffPool	32.9	34.4	20.0	23.5	20.2	26.3	22.1	38.3	35.9	41.8	-	-	-	-
MinCut	35.8	25.0	25.9	20.1	25.4	15.8	-	-	-	-	48.3	24.9	36.0	27.1
Ortho	38.4	26.6	26.1	20.5	20.3	13.9	-	-	-	-	44.7	23.7	35.6	26.7
DMoN	48.8	48.8	33.7	43.2	29.8	33.9	49.3	45.4	63.3	61.0	56.7	42.4	37.6	45.7
DGCluster	62.1	54.5	41.0	32.2	32.6	34.6	60.4	52.2	77.3	75.9	65.7	49.2	31.2	32.4
Clustering Time	93.6ms		119.6ms		405.5ms		286.1ms		204.6ms		547.4ms		2.7s	
NID$_{DGCluster}$	**70.5**	**73.9**	**54.1**	**63.3**	**40.6**	**50.9**	**62.1**	**58.2**	75.6	75.4	**69.8**	**65.4**	32.4	35.6
Clustering Time	78.3ms		77.2ms		292.5ms		223.6ms		140.6ms		442.0ms		1.8s	

Table 6: Node classification results in unsupervised representation learning (%).

Metric	Cora Accuracy↑	CiteSeer Accuracy↑	PubMed Accuracy↑	dim
GAE	71.5 ±0.4	65.8 ±0.4	72.1 ±0.5	16
DGI	82.3 ±0.6	71.8 ±0.7	76.8 ±0.6	512
MVGRL	83.5 ±0.4	73.3 ±0.5	80.1 ±0.7	512
InfoGCL	83.5 ±0.3	73.5 ±0.4	79.1 ±0.2	512
CCA-SSG	84.0 ±0.4	73.1 ±0.3	81.0 ±0.4	512
MLP	57.8 ±0.5	54.7 ±0.4	73.3 ±0.6	500
GraphMAE	84.2 ±0.4	73.4 ±0.4	81.1 ±0.4	512
NID$_{MAE}$	80.8 ±0.7	**74.2 ±0.6**	76.4 ±0.8	6

Table 7: Graph classification results in unsupervised representation learning on TUDataset; Accuracy (%).

	NCI1	PROTEINS	DD	MUTAG	COLLAB	RDT-B	RDT-M5K	IMDB-B
# graphs	4,110	1,113	1,178	188	5,000	2,000	4,999	1,000
Avg. # nodes	29.8	39.1	284.3	17.9	74.5	429.7	508.5	19.8
InfoGraph	76.2 ±1.0	74.4 ±0.3	72.8 ±1.7	89.0 ±1.1	70.6 ±1.1	82.5 ±1.4	53.4 ±1.0	73.0 ±0.8
MVGRL	-	-	-	89.7 ±1.1	-	84.5 ±0.6	-	74.2 ±0.7
JOAO	78.3 ±0.5	74.0 ±1.1	77.4 ±1.1	87.6 ±0.7	69.3 ±0.3	86.4 ±1.4	56.0 ±0.2	70.8 ±0.2
GraphMAE	80.4 ±0.3	75.3 ±0.4	-	88.1 ±1.3	80.3 ±0.5	88.0 ±0.2	-	75.5 ±0.6
AD-GCL	69.6 ±0.5	73.5 ±0.6	74.4 ±0.5	-	73.3 ±0.6	85.5 ±0.7	53.0 ±0.8	71.5 ±1.0
GraphCL	77.8 ±0.4	74.3 ±0.4	78.6 ±0.4	86.8 ±1.3	71.3 ±1.1	89.5 ±0.8	55.9 ±0.2	71.1 ±0.4
NID$_{CL}$	75.9 ±0.6	75.1 ±0.5	77.8 ±1.1	88.6 ±1.7	76.9 ±0.3	**90.7 ±0.9**	55.0 ±0.5	72.3 ±1.2
AutoGCL	82.0 ±0.2	75.8 ±0.3	77.5 ±0.6	88.6 ±1.0	70.1 ±0.6	88.5 ±1.4	56.7 ±0.1	73.3 ±0.4
NID$_{AutoGCL}$	78.2 ±1.5	**75.9 ±0.6**	77.2 ±0.9	**90.4 ±0.8**	74.5 ±1.1	89.8 ±0.7	54.2 ±0.6	72.4 ±0.8

Link Prediction, Table 4. We test NID on 4 well-known link prediction benchmarks: Cora, Citeseer, Pubmed and ogbl-collab from the OGB (Hu et al., 2020), following the data splits, evaluation metrics and baselines specified by the NCN (Wang et al., 2023c). The results in Table 4 highlight NID's competitive performance, demonstrating both high accuracy and efficiency in link prediction tasks.

4.1.2 SELF-SUPERVISED NODE IDS FOR UNSUPERVISED REPRESENTATION LEARNING

Attributed Graph Clustering, Table 5. Attributed graph clustering (Cai et al., 2018) focuses on clustering nodes in an attributed graph, where each node is associated with a set of feature attributes. DGCluster (Bhowmick et al., 2024), utilizes GNNs to optimize modularity for this task, representing the latest SOTA method. In this study, we apply the NID framework within DGCluster, quantizing the embeddings learned by the GCN in DGCluster into node IDs, which are then used for clustering. We select 7 datasets from DGCluster and adopt all experimental settings and baselines as described in DGCluster (Bhowmick et al., 2024). As demonstrated in Table 5, **NID**$_{DGCluster}$ outperforms all baseline models by a considerable margin on 5 datasets and achieves significantly faster runtime on 7 datasets due to the reduced dimensionality of our node IDs.

Node Classification, Table 6. We evaluate the performance of our NID on three standard benchmarks: Cora, CiteSeer, and PubMed (Yang et al., 2016). For this purpose, we employ GraphMAE to provide graph learning objective during the training of node IDs. Specifically, we train a 2-layer GAT following the GraphMAE without supervision, resulting in the generation of 6-dim node IDs, denoted as **NID**$_{MAE}$. Subsequently, we train an MLP and report the mean accuracy on the test nodes. For the evaluation protocol, we follow all the experimental settings used in GraphMAE (Hou et al., 2022), including data splits and evaluation metrics, using all baselines reported by Hou et al. (2022). Table 6 lists the results. MLP refers to predictions made directly on the initial node features. Notably, **NID**$_{MAE}$ achieves competitive results in comparison to SOTA self-supervised approaches, and even surpasses all other approaches on CiteSeer. Remarkably, our node IDs are comprised of only 6 discrete codes, with each code having a maximum of 32 possible values. This demonstrates that our NID effectively compresses the node's representation into a concise yet information-rich ID.

Graph Classification, Tables 7 and 13. We evaluate our NID framework on 8 datasets from TUDataset (Morris et al., 2020): NCI1, PROTEINS, DD, MUTAG, COLLAB, REDDIT-B, REDDIT-M5K, and IMDB-B, utilizing two different methods, GraphCL (You et al., 2020) and AutoGCL (Yin et al., 2022), as graph learning objectives to guide node IDs pre-training. Specifically, using

Table 8: Comparison of codebook usage rates (%).

Usage rate↑	Cora	CiteSeer	PubMed
VQGraph	1.3	0.8	18.1
NID$_{\text{GCN}}$	84.7	97.9	79.1
NID$_{\text{GCN}(M=1)}$	83.3	81.3	78.1

Table 9: Average GEDs of 1-hop subgraphs among nodes.

GEDs↓	Cora	CiteSeer	PubMed
Random	7.21	4.83	9.61
VQGraph	6.85	4.73	9.03
NID$_{\text{GCN}}$	6.15	3.89	6.22

Table 10: Accuracy vs Inference Time.

Metric	Computer		ogbn-products	
	Acc↑	Time↓	Acc↑	Time↓
GCN	93.78	119.6ms	82.33	12.8s
SAGE	93.59	95.7ms	83.27	11.9s
VQGraph	90.28	1.4ms	79.17	1.6ms
NID$_{\text{SAGE}}$	**93.32**	**0.5ms**	81.83	**0.7ms**
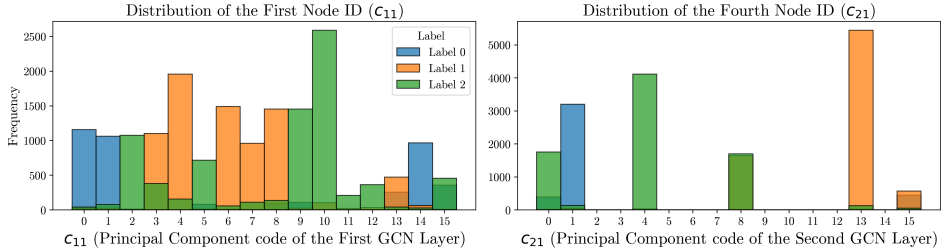
Figure 5: Codeword distributions of c_{11} and c_{21} in PubMed colored by the ground-truth labels.

GraphCL as an example, we employ a GIN with the default settings from GraphCL as the GNN-based encoder, denoted as **NID**$_{\text{CL}}$. We adhere to the evaluation protocol outlined in GraphCL (You et al., 2020). The results are presented in Table 7, where NID outperforms all baselines on 3 out of 8 datasets. This performance demonstrates that our NID is capable of learning meaningful information and demonstrates potential for application in graph-level tasks. Additional linear probing results on MoleculeNet datasets (Wu et al., 2018) are discussed in App. D, showing consistent findings.

4.2 Analysis of Node IDs

High Codebook Usage, Table 8. We calculate the codebook usage rates for VQGraph tokenizer and NID. We find that VQGraph suffers from severe codebook collapse (Dhariwal et al., 2020), where the majority of nodes are quantized into a small number of code vectors, leaving most of the codebook unused. In contrast, our NID achieves high codebook usage, effectively avoiding codebook collapse.

Qualitative Analysis, Figures 5, 7, 8. We analyze the supervised node IDs of **NID**$_{\text{GCN}}$ for the PubMed dataset, depicted in Figures 5 & 7. The number of RVQ levels M is set to 3, and the MPNN layers L is set to 2, with a codebook size K of 16. For a given node ID $(c_{11}, c_{12}, c_{13}, c_{21}, c_{22}, c_{23})$ of a node, $0 \leq c_{lm} \leq 15$. The codes c_{11} and c_{21} capture the high-level information of the first and second MPNN layers, respectively. We present the distribution of c_{11} and c_{21} according to different labels. For instance, $c_{11} = 10$ generally corresponds to label "2". Similarly, the majority of nodes with $c_{21} = 13$ are labeled "1". Our node IDs have overlapping codewords for similar labels, allowing the model to effectively share knowledge from similar nodes in the dataset.

Subgraph Retrieval, Table 9. We conduct node-centered subgraph retrieval using the supervised node IDs of **NID**$_{\text{GCN}}$ on Cora, CiteSeer and PubMed. We identify the five nodes closest to a query node based on Hamming distances between their node IDs, then compute the average graph edit distance (GED) between the 1-hop subgraph of the query node and the 1-hop subgraphs of these five nodes. The average GED across all nodes is detailed in Table 9. For comparison, we also calculate the GEDs using the VQGraph tokens and the randomly selected nodes. The results show that node IDs perform better in subgraph retrieval, with similar IDs more likely to exhibit similar structures.

Acceleration in Inference Time, Table 10. We show the supervised node classification accuracy and model inference time on the Computer and ogbn-products datasets in Table 10. Our results indicate that we achieve the high accuracy of 81% and 93% while maintaining a fast inference time of 0.5ms and 0.7ms, respectively. Since the ogbn-products dataset contains over sixty million edges, graph loading is very slow. However, under the NID framework, we reduce the SAGE inference time from 11.9s to 0.7ms, demonstrating a significant inference speedup of our approach in large networks.

Ablation Study of the Codebook Size K, RVQ Level M and MPNNs Layer L, Figure 6. First, we examine the influence of the codebook size K. The optimal K varies across different graphs; however, generally, $K \leq 16$ yields the best performance on most datasets. A larger codebook size may lead to codebook collapse, impairing performance. Second, regarding the RVQ level M, we
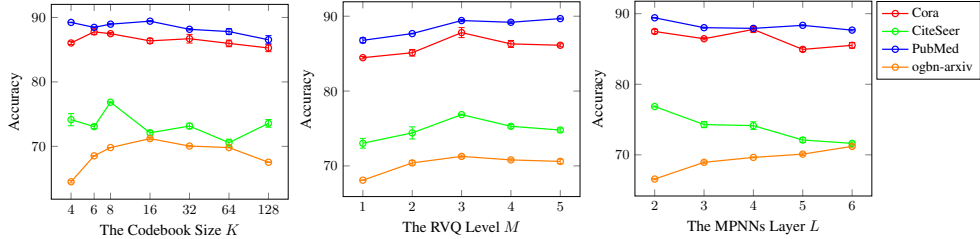
Figure 6: Impact of codebook size, RVQ levels, and MPNN layers on node classification using $\textbf{NID}_{\text{GCN}}$.

find that $M = 3$ performs the best, which validates our fixed choice. Notably, when $M = 1$, RVQ degenerates into VQ, which leads to decreased performance. Third, the number of MPNN layers required also differs based on the graph size. For instance, smaller graphs like CiteSeer perform well with just 2 layers, while larger graphs, such as ogbn-arxiv, may require more than 6 layers.

5 RELATED WORKS

Inference Acceleration for GNNs. GNNs are the preferred method for representation learning on graph-structured data but suffer from decreased inference efficiency as graph size and the number of layers increase, especially in real-time and resource-limited scenarios (Kaler et al., 2022). To address this issue, three main strategies are employed (Ma et al., 2024): knowledge distillation, model pruning, and model quantization. Knowledge distillation includes GNN-to-GNN methods (Yan et al., 2020; Yang et al., 2022) and GNN-to-MLP approaches (Hu et al., 2021; Yang et al., 2024)). Model pruning methods include UGS (Chen et al., 2021) and Snowflake (Wang et al., 2023a)). Lastly, model quantization methods include VQ-GNN (Ding et al., 2021) and QLR (Wang et al., 2023b)).

Graph Tokenization. In graph representation learning, significant strides have been made to vectorize structured data for downstream machine learning applications (Chami et al., 2022). Early pioneering efforts, such as DeepWalk (Perozzi et al., 2014) and node2vec (Grover & Leskovec, 2016), popularized the concept of node embedding learning. Subsequently, GNNs have been extensively used as encoders to learn embeddings for graph tokens including nodes, edges, and (sub)graphs, with applications across various domains including molecular motifs (Liu et al., 2024d; Rong et al., 2020; Zhang et al., 2021c; Luo et al., 2023a), recommendation systems (Tang et al., 2024; Liu et al., 2024a), and knowledge graphs (Tang et al., 2023; Lou et al., 2023; Liang et al., 2024b; 2023; 2024a). The emergence of Large Language Models (LLMs) has spurred recent explorations into graph tokenization. Works like InstructGLM (Ye et al., 2023), GraphText (Zhao et al., 2023), and GPT4Graph (Guo et al., 2023) use natural language descriptions of graphs as tokens inputted to LLMs. Additionally, GraphToken (Perozzi et al., 2024) integrates graph tokens generated by GNNs with textual tokens to explicitly represent structured data for LLMs.

Differences between Our NID and VQGraph. We clarify that our NID framework is fundamentally different from VQGraph (Yang et al., 2024), even though both approaches utilize VQ techniques to tokenize nodes as discrete codes. VQGraph uses VQ-VAE (Van Den Oord et al., 2017) to obtain soft code assignments, which serve as targets to aid the GNN-to-MLP distillation process. However, similar to other GNN-to-MLP methods, VQGraph lacks the capability to generate interpretable node representations, limiting its application to supervised node classification. In contrast, our NID framework is designed to learn compact discrect node representations in both supervised and unsupervised manners, enabling its use across a wide range of downstream tasks. Moreover, VQGraph employs a sizable codebook for tokenization, with a capacity comparable to the size of the input graph, leading to codebook collapse (Tab. 8). In contrast, our NID tokenizer utilizes multiple, small-sized codebooks to achieve a large representational capacity and effectively prevents codebook collapse.

6 CONCLUSIONS

We have both empirically and theoretically validated the feasibility of learning highly compact, discrete, and interpretable codes (node IDs) as effective node representations for efficient graph learning. Our proposed NID framework can be seamlessly integrated with state-of-the-art unsupervised and supervised GNN methods to further enhance their performance. These findings have the potential to facilitate graph tokenization and applications involving large language models.

REFERENCES

Mohammad Sadegh Akhondzadeh, Vijay Lingam, and Aleksandar Bojchevski. Probing graph representations. In Francisco Ruiz, Jennifer Dy, and Jan-Willem van de Meent (eds.), *Proceedings of The 26th International Conference on Artificial Intelligence and Statistics*, volume 206 of *Proceedings of Machine Learning Research*, pp. 11630–11649. PMLR, 25–27 Apr 2023. URL https://proceedings.mlr.press/v206/akhondzadeh23a.html.

Albert-László Barabási and Réka Albert. Emergence of scaling in random networks. *science*, 286 (5439):509–512, 1999.

Aritra Bhowmick, Mert Kosan, Zexi Huang, Ambuj Singh, and Sourav Medya. Dgcluster: A neural framework for attributed graph clustering via modularity maximization. In *Proceedings of the AAAI Conference on Artificial Intelligence*, volume 38, pp. 11069–11077, 2024.

Filippo Maria Bianchi, Daniele Grattarola, and Cesare Alippi. Spectral clustering with graph neural networks for graph pooling. In *International conference on machine learning*, pp. 874–883. PMLR, 2020.

Deyu Bo, Xiao Wang, Chuan Shi, Meiqi Zhu, Emiao Lu, and Peng Cui. Structural deep clustering network. In *Proceedings of the web conference 2020*, pp. 1400–1410, 2020.

Deyu Bo, Chuan Shi, Lele Wang, and Renjie Liao. Specformer: Spectral graph neural networks meet transformers. *arXiv preprint arXiv:2303.01028*, 2023.

Joan Bruna, Wojciech Zaremba, Arthur Szlam, and Yann LeCun. Spectral networks and locally connected networks on graphs. *arXiv preprint arXiv:1312.6203*, 2013.

Hongyun Cai, Vincent W Zheng, and Kevin Chen-Chuan Chang. A comprehensive survey of graph embedding: Problems, techniques, and applications. *IEEE transactions on knowledge and data engineering*, 30(9):1616–1637, 2018.

Benjamin Paul Chamberlain, Sergey Shirobokov, Emanuele Rossi, Fabrizio Frasca, Thomas Markovich, Nils Yannick Hammerla, Michael M Bronstein, and Max Hansmire. Graph neural networks for link prediction with subgraph sketching. In *The eleventh international conference on learning representations*, 2022.

Ines Chami, Sami Abu-El-Haija, Bryan Perozzi, Christopher Ré, and Kevin Murphy. Machine learning on graphs: A model and comprehensive taxonomy. *Journal of Machine Learning Research*, 23 (89):1–64, 2022.

Chih-Chung Chang and Chih-Jen Lin. Libsvm: a library for support vector machines. *ACM transactions on intelligent systems and technology (TIST)*, 2(3):1–27, 2011.

Dexiong Chen, Leslie O'Bray, and Karsten Borgwardt. Structure-aware transformer for graph representation learning. In *International Conference on Machine Learning*, pp. 3469–3489. PMLR, 2022a.

Jinsong Chen, Kaiyuan Gao, Gaichao Li, and Kun He. Nagphormer: A tokenized graph transformer for node classification in large graphs. In *The Eleventh International Conference on Learning Representations*, 2022b.

Tianlong Chen, Yongduo Sui, Xuxi Chen, Aston Zhang, and Zhangyang Wang. A unified lottery ticket hypothesis for graph neural networks. In *International conference on machine learning*, pp. 1695–1706. PMLR, 2021.

Eli Chien, Jianhao Peng, Pan Li, and Olgica Milenkovic. Adaptive universal generalized pagerank graph neural network. In *International Conference on Learning Representations*, 2020.

Michaël Defferrard, Xavier Bresson, and Pierre Vandergheynst. Convolutional neural networks on graphs with fast localized spectral filtering. *Advances in neural information processing systems*, 29, 2016.

Chenhui Deng, Zichao Yue, and Zhiru Zhang. Polynormer: Polynomial-expressive graph transformer in linear time. *arXiv preprint arXiv:2403.01232*, 2024.

Prafulla Dhariwal, Heewoo Jun, Christine Payne, Jong Wook Kim, Alec Radford, and Ilya Sutskever. Jukebox: A generative model for music. *arXiv preprint arXiv:2005.00341*, 2020.

Mucong Ding, Kezhi Kong, Jingling Li, Chen Zhu, John Dickerson, Furong Huang, and Tom Goldstein. Vq-gnn: A universal framework to scale up graph neural networks using vector quantization. *Advances in Neural Information Processing Systems*, 34:6733–6746, 2021.

Vijay Prakash Dwivedi and Xavier Bresson. A generalization of transformer networks to graphs. *arXiv preprint arXiv:2012.09699*, 2020.

Vijay Prakash Dwivedi, Anh Tuan Luu, Thomas Laurent, Yoshua Bengio, and Xavier Bresson. Graph neural networks with learnable structural and positional representations. In *International Conference on Learning Representations*, 2021.

Vijay Prakash Dwivedi, Ladislav Rampášek, Mikhail Galkin, Ali Parviz, Guy Wolf, Anh Tuan Luu, and Dominique Beaini. Long range graph benchmark. *arXiv preprint arXiv:2206.08164*, 2022.

Vijay Prakash Dwivedi, Yozen Liu, Anh Tuan Luu, Xavier Bresson, Neil Shah, and Tong Zhao. Graph transformers for large graphs. *arXiv preprint arXiv:2312.11109*, 2023.

Matthias Fey and Jan Eric Lenssen. Fast graph representation learning with pytorch geometric. *arXiv preprint arXiv:1903.02428*, 2019.

Santo Fortunato. Community detection in graphs. *Physics reports*, 486(3-5):75–174, 2010.

Santo Fortunato and Darko Hric. Community detection in networks: A user guide. *Physics reports*, 659:1–44, 2016.

Johannes Gasteiger, Aleksandar Bojchevski, and Stephan Günnemann. Predict then propagate: Graph neural networks meet personalized pagerank. *arXiv preprint arXiv:1810.05997*, 2018.

Justin Gilmer, Samuel S Schoenholz, Patrick F Riley, Oriol Vinyals, and George E Dahl. Neural message passing for quantum chemistry. In *International conference on machine learning*, pp. 1263–1272. PMLR, 2017.

Robert Gray. Vector quantization. *IEEE Assp Magazine*, 1(2):4–29, 1984.

Aditya Grover and Jure Leskovec. node2vec: Scalable feature learning for networks. In *Proceedings of the 22nd ACM SIGKDD international conference on Knowledge discovery and data mining*, pp. 855–864, 2016.

Jiayan Guo, Lun Du, and Hengyu Liu. Gpt4graph: Can large language models understand graph structured data? an empirical evaluation and benchmarking. *arXiv preprint arXiv:2305.15066*, 2023.

Will Hamilton, Zhitao Ying, and Jure Leskovec. Inductive representation learning on large graphs. *Advances in neural information processing systems*, 30, 2017.

Kaveh Hassani and Amir Hosein Khasahmadi. Contrastive multi-view representation learning on graphs. In *International conference on machine learning*, pp. 4116–4126. PMLR, 2020.

Xiaoxin He, Bryan Hooi, Thomas Laurent, Adam Perold, Yann LeCun, and Xavier Bresson. A generalization of vit/mlp-mixer to graphs. In *International Conference on Machine Learning*, pp. 12724–12745. PMLR, 2023.

Van Thuy Hoang, O Lee, et al. A survey on structure-preserving graph transformers. *arXiv preprint arXiv:2401.16176*, 2024.

Zhenyu Hou, Xiao Liu, Yukuo Cen, Yuxiao Dong, Hongxia Yang, Chunjie Wang, and Jie Tang. Graphmae: Self-supervised masked graph autoencoders. In *Proceedings of the 28th ACM SIGKDD Conference on Knowledge Discovery and Data Mining*, pp. 594–604, 2022.

Weihua Hu, Matthias Fey, Marinka Zitnik, Yuxiao Dong, Hongyu Ren, Bowen Liu, Michele Catasta, and Jure Leskovec. Open graph benchmark: Datasets for machine learning on graphs. *Advances in neural information processing systems*, 33:22118–22133, 2020.

Weihua Hu*, Bowen Liu*, Joseph Gomes, Marinka Zitnik, Percy Liang, Vijay Pande, and Jure Leskovec. Strategies for pre-training graph neural networks. In *International Conference on Learning Representations*, 2020. URL https://openreview.net/forum?id=HJlWWJSFDH.

Yang Hu, Haoxuan You, Zhecan Wang, Zhicheng Wang, Erjin Zhou, and Yue Gao. Graph-mlp: Node classification without message passing in graph. *arXiv preprint arXiv:2106.04051*, 2021.

Zhihao Jia, Sina Lin, Rex Ying, Jiaxuan You, Jure Leskovec, and Alex Aiken. Redundancy-free computation for graph neural networks. In *Proceedings of the 26th ACM SIGKDD International Conference on Knowledge Discovery & Data Mining*, pp. 997–1005, 2020.

Biing-Hwang Juang and A Gray. Multiple stage vector quantization for speech coding. In *ICASSP'82. IEEE International Conference on Acoustics, Speech, and Signal Processing*, volume 7, pp. 597–600. IEEE, 1982.

Tim Kaler, Nickolas Stathas, Anne Ouyang, Alexandros-Stavros Iliopoulos, Tao Schardl, Charles E Leiserson, and Jie Chen. Accelerating training and inference of graph neural networks with fast sampling and pipelining. *Proceedings of Machine Learning and Systems*, 4:172–189, 2022.

Jinwoo Kim, Dat Nguyen, Seonwoo Min, Sungjun Cho, Moontae Lee, Honglak Lee, and Seunghoon Hong. Pure transformers are powerful graph learners. *Advances in Neural Information Processing Systems*, 35:14582–14595, 2022.

Diederik P Kingma and Jimmy Ba. Adam: A method for stochastic optimization. *arXiv preprint arXiv:1412.6980*, 2014.

Thomas N Kipf and Max Welling. Variational graph auto-encoders. *arXiv preprint arXiv:1611.07308*, 2016.

Thomas N. Kipf and Max Welling. Semi-supervised classification with graph convolutional networks. In *International Conference on Learning Representations*, 2017. URL https://openreview.net/forum?id=SJU4ayYgl.

Kezhi Kong, Jiuhai Chen, John Kirchenbauer, Renkun Ni, C. Bayan Bruss, and Tom Goldstein. GOAT: A global transformer on large-scale graphs. In Andreas Krause, Emma Brunskill, Kyunghyun Cho, Barbara Engelhardt, Sivan Sabato, and Jonathan Scarlett (eds.), *Proceedings of the 40th International Conference on Machine Learning*, volume 202 of *Proceedings of Machine Learning Research*, pp. 17375–17390. PMLR, 23–29 Jul 2023. URL https://proceedings.mlr.press/v202/kong23a.html.

Ioannis Konstas, Vassilios Stathopoulos, and Joemon M Jose. On social networks and collaborative recommendation. In *Proceedings of the 32nd international ACM SIGIR conference on Research and development in information retrieval*, pp. 195–202, 2009.

Devin Kreuzer, Dominique Beaini, Will Hamilton, Vincent Létourneau, and Prudencio Tossou. Rethinking graph transformers with spectral attention. *Advances in Neural Information Processing Systems*, 34:21618–21629, 2021.

Weirui Kuang, WANG Zhen, Yaliang Li, Zhewei Wei, and Bolin Ding. Coarformer: Transformer for large graph via graph coarsening. 2021.

Doyup Lee, Chiheon Kim, Saehoon Kim, Minsu Cho, and Wook-Shin Han. Autoregressive image generation using residual quantization. In *Proceedings of the IEEE/CVF Conference on Computer Vision and Pattern Recognition*, pp. 11523–11532, 2022.

Jure Leskovec and Andrej Krevl. Snap datasets: Stanford large network dataset collection. 2014. 2016.

Hongkang Li, Meng Wang, Tengfei Ma, Sijia Liu, ZAIXI ZHANG, and Pin-Yu Chen. What improves the generalization of graph transformers? a theoretical dive into the self-attention and positional encoding. In *Forty-first International Conference on Machine Learning*, 2024. URL https://openreview.net/forum?id=mJhXlsZzzE.

Qimai Li, Zhichao Han, and Xiao-Ming Wu. Deeper insights into graph convolutional networks for semi-supervised learning. In *Thirty-Second AAAI conference on artificial intelligence*, 2018.

Qimai Li, Xiao-Ming Wu, Han Liu, Xiaotong Zhang, and Zhichao Guan. Label efficient semi-supervised learning via graph filtering. In *Proceedings of the IEEE/CVF conference on computer vision and pattern recognition*, pp. 9582–9591, 2019.

Ke Liang, Yue Liu, Sihang Zhou, Wenxuan Tu, Yi Wen, Xihong Yang, Xiangjun Dong, and Xinwang Liu. Knowledge graph contrastive learning based on relation-symmetrical structure. *IEEE Transactions on Knowledge and Data Engineering*, 36(1):226–238, 2023.

Ke Liang, Lingyuan Meng, Hao Li, Meng Liu, Siwei Wang, Sihang Zhou, Xinwang Liu, and Kunlun He. Mgksite: Multi-modal knowledge-driven site selection via intra and inter-modal graph fusion. *IEEE Transactions on Multimedia*, 2024a.

Ke Liang, Lingyuan Meng, Meng Liu, Yue Liu, Wenxuan Tu, Siwei Wang, Sihang Zhou, Xinwang Liu, Fuchun Sun, and Kunlun He. A survey of knowledge graph reasoning on graph types: Static, dynamic, and multi-modal. *IEEE Transactions on Pattern Analysis and Machine Intelligence*, 2024b.

Derek Lim, Felix Hohne, Xiuyu Li, Sijia Linda Huang, Vaishnavi Gupta, Omkar Bhalerao, and Ser Nam Lim. Large scale learning on non-homophilous graphs: New benchmarks and strong simple methods. *Advances in Neural Information Processing Systems*, 34:20887–20902, 2021.

Chuang Liu, Yibing Zhan, Xueqi Ma, Liang Ding, Dapeng Tao, Jia Wu, and Wenbin Hu. Gapformer: Graph transformer with graph pooling for node classification. In *Proceedings of the Thirty-Second International Joint Conference on Artificial Intelligence, IJCAI*, pp. 2196–2205, 2023.

Han Liu, Yinwei Wei, Xuemeng Song, Weili Guan, Yuan-Fang Li, and Liqiang Nie. Mmgrec: Multimodal generative recommendation with transformer model. *arXiv preprint arXiv:2404.16555*, 2024a.

Qijiong Liu, Xiaoyu Dong, Jiaren Xiao, Nuo Chen, Hengchang Hu, Jieming Zhu, Chenxu Zhu, Tetsuya Sakai, and Xiao-Ming Wu. Vector quantization for recommender systems: A review and outlook. *arXiv preprint arXiv:2405.03110*, 2024b.

Qijiong Liu, Hengchang Hu, Jiahao Wu, Jieming Zhu, Min-Yen Kan, and Xiao-Ming Wu. Discrete semantic tokenization for deep ctr prediction. *arXiv preprint arXiv:2403.08206*, 2024c.

Xiao Liu, Fanjin Zhang, Zhenyu Hou, Li Mian, Zhaoyu Wang, Jing Zhang, and Jie Tang. Self-supervised learning: Generative or contrastive. *IEEE transactions on knowledge and data engineering*, 35(1):857–876, 2021.

Zhiyuan Liu, Yaorui Shi, An Zhang, Enzhi Zhang, Kenji Kawaguchi, Xiang Wang, and Tat-Seng Chua. Rethinking tokenizer and decoder in masked graph modeling for molecules. *Advances in Neural Information Processing Systems*, 36, 2024d.

Yunzhong Lou, Xueyang Li, Haotian Chen, and Xiangdong Zhou. Brep-bert: Pre-training boundary representation bert with sub-graph node contrastive learning. In *Proceedings of the 32nd ACM International Conference on Information and Knowledge Management*, pp. 1657–1666, 2023.

Linyuan Lü and Tao Zhou. Link prediction in complex networks: A survey. *Physica A: statistical mechanics and its applications*, 390(6):1150–1170, 2011.

Yuankai Luo, Lei Shi, and Veronika Thost. Improving self-supervised molecular representation learning using persistent homology. In *Thirty-seventh Conference on Neural Information Processing Systems*, 2023a. URL https://openreview.net/forum?id=wEiUGpcr0M.

Yuankai Luo, Lei Shi, Mufan Xu, Yuwen Ji, Fengli Xiao, Chunming Hu, and Zhiguang Shan. Impact-oriented contextual scholar profiling using self-citation graphs. *arXiv preprint arXiv:2304.12217*, 2023b.

Yuankai Luo, Hongkang Li, Lei Shi, and Xiao-Ming Wu. Enhancing graph transformers with hierarchical distance structural encoding. In *The Thirty-eighth Annual Conference on Neural Information Processing Systems*, 2024a. URL https://openreview.net/forum?id=U4KldRgoph.

Yuankai Luo, Lei Shi, and Xiao-Ming Wu. Classic gnns are strong baselines: Reassessing gnns for node classification. *arXiv preprint arXiv:2406.08993*, 2024b.

Yuankai Luo, Veronika Thost, and Lei Shi. Transformers over directed acyclic graphs. *Advances in Neural Information Processing Systems*, 36, 2024c.

Yuankai Luo, Lei Shi, and Xiao-Ming Wu. Unlocking the potential of classic gnns for graph-level tasks: Simple architectures meet excellence. *arXiv preprint arXiv:2502.09263*, 2025a.

Yuankai Luo, Xiao-Ming Wu, and Hao Zhu. Beyond random masking: When dropout meets graph convolutional networks. In *The Thirteenth International Conference on Learning Representations*, 2025b. URL https://openreview.net/forum?id=PwxYoMvmvy.

Liheng Ma, Chen Lin, Derek Lim, Adriana Romero-Soriano, Puneet K Dokania, Mark Coates, Philip Torr, and Ser-Nam Lim. Graph inductive biases in transformers without message passing. *arXiv preprint arXiv:2305.17589*, 2023.

Lu Ma, Zeang Sheng, Xunkai Li, Xinyi Gao, Zhezheng Hao, Ling Yang, Wentao Zhang, and Bin Cui. Acceleration algorithms in gnns: A survey. *arXiv preprint arXiv:2405.04114*, 2024.

James MacQueen et al. Some methods for classification and analysis of multivariate observations. In *Proceedings of the fifth Berkeley symposium on mathematical statistics and probability*, volume 1, pp. 281–297. Oakland, CA, USA, 1967.

Julieta Martinez, Holger H Hoos, and James J Little. Stacked quantizers for compositional vector compression. *arXiv preprint arXiv:1411.2173*, 2014.

Julian McAuley, Rahul Pandey, and Jure Leskovec. Inferring networks of substitutable and complementary products. In *Proceedings of the 21th ACM SIGKDD international conference on knowledge discovery and data mining*, pp. 785–794, 2015.

Fabian Mentzer, David Minnen, Eirikur Agustsson, and Michael Tschannen. Finite scalar quantization: VQ-VAE made simple. In *The Twelfth International Conference on Learning Representations*, 2024. URL https://openreview.net/forum?id=8ishA3LxN8.

Péter Mernyei and Cătălina Cangea. Wiki-cs: A wikipedia-based benchmark for graph neural networks. *arXiv preprint arXiv:2007.02901*, 2020.

Christopher Morris, Nils M Kriege, Franka Bause, Kristian Kersting, Petra Mutzel, and Marion Neumann. Tudataset: A collection of benchmark datasets for learning with graphs. *arXiv preprint arXiv:2007.08663*, 2020.

Luis Müller, Mikhail Galkin, Christopher Morris, and Ladislav Rampášek. Attending to graph transformers. *arXiv preprint arXiv:2302.04181*, 2023.

Hongbin Pei, Bingzhe Wei, Kevin Chen-Chuan Chang, Yu Lei, and Bo Yang. Geom-gcn: Geometric graph convolutional networks. In *International Conference on Learning Representations*, 2019.

Tiago P Peixoto. Efficient monte carlo and greedy heuristic for the inference of stochastic block models. *Physical Review E*, 89(1):012804, 2014.

Bryan Perozzi, Rami Al-Rfou, and Steven Skiena. Deepwalk: Online learning of social representations. In *Proceedings of the 20th ACM SIGKDD international conference on Knowledge discovery and data mining*, pp. 701–710, 2014.

Bryan Perozzi, Bahare Fatemi, Dustin Zelle, Anton Tsitsulin, Mehran Kazemi, Rami Al-Rfou, and Jonathan Halcrow. Let your graph do the talking: Encoding structured data for llms. *arXiv preprint arXiv:2402.05862*, 2024.

Oleg Platonov, Denis Kuznedelev, Michael Diskin, Artem Babenko, and Liudmila Prokhorenkova. A critical look at the evaluation of gnns under heterophily: Are we really making progress? *arXiv preprint arXiv:2302.11640*, 2023.

Haohao Qu, Wenqi Fan, Zihuai Zhao, and Qing Li. Tokenrec: Learning to tokenize id for llm-based generative recommendation. *arXiv preprint arXiv:2406.10450*, 2024.

Shashank Rajput, Nikhil Mehta, Anima Singh, Raghunandan Hulikal Keshavan, Trung Vu, Lukasz Heldt, Lichan Hong, Yi Tay, Vinh Tran, Jonah Samost, et al. Recommender systems with generative retrieval. *Advances in Neural Information Processing Systems*, 36, 2024.

Ladislav Rampášek, Mikhail Galkin, Vijay Prakash Dwivedi, Anh Tuan Luu, Guy Wolf, and Dominique Beaini. Recipe for a general, powerful, scalable graph transformer. *arXiv preprint arXiv:2205.12454*, 2022.

Bharath Ramsundar, Peter Eastman, Patrick Walters, and Vijay Pande. *Deep learning for the life sciences: applying deep learning to genomics, microscopy, drug discovery, and more*. O'Reilly Media, 2019.

Ali Razavi, Aaron Van den Oord, and Oriol Vinyals. Generating diverse high-fidelity images with vq-vae-2. *Advances in neural information processing systems*, 32, 2019.

Yu Rong, Yatao Bian, Tingyang Xu, Weiyang Xie, Ying Wei, Wenbing Huang, and Junzhou Huang. Self-supervised graph transformer on large-scale molecular data. *Advances in neural information processing systems*, 33:12559–12571, 2020.

Benedek Rozemberczki, Carl Allen, and Rik Sarkar. Multi-scale attributed node embedding. *Journal of Complex Networks*, 9(2):cnab014, 2021.

Oleksandr Shchur and Stephan Günnemann. Overlapping community detection with graph neural networks. *arXiv preprint arXiv:1909.12201*, 2019.

Hamed Shirzad, Ameya Velingker, Balaji Venkatachalam, Danica J Sutherland, and Ali Kemal Sinop. Exphormer: Sparse transformers for graphs. *arXiv preprint arXiv:2303.06147*, 2023.

Kihyuk Sohn. Improved deep metric learning with multi-class n-pair loss objective. *Advances in neural information processing systems*, 29, 2016.

Fan-Yun Sun, Jordan Hoffmann, Vikas Verma, and Jian Tang. Infograph: Unsupervised and semi-supervised graph-level representation learning via mutual information maximization. *arXiv preprint arXiv:1908.01000*, 2019.

Susheel Suresh, Pan Li, Cong Hao, and Jennifer Neville. Adversarial graph augmentation to improve graph contrastive learning. *Advances in Neural Information Processing Systems*, 34:15920–15933, 2021.

Jiabin Tang, Yuhao Yang, Wei Wei, Lei Shi, Lixin Su, Suqi Cheng, Dawei Yin, and Chao Huang. Graphgpt: Graph instruction tuning for large language models. *arXiv preprint arXiv:2310.13023*, 2023.

Jiabin Tang, Yuhao Yang, Wei Wei, Lei Shi, Long Xia, Dawei Yin, and Chao Huang. Higpt: Heterogeneous graph language model. *arXiv preprint arXiv:2402.16024*, 2024.

Yijun Tian, Chuxu Zhang, Zhichun Guo, Xiangliang Zhang, and Nitesh Chawla. Learning mlps on graphs: A unified view of effectiveness, robustness, and efficiency. In *The Eleventh International Conference on Learning Representations*, 2022.

Yijun Tian, Shichao Pei, Xiangliang Zhang, Chuxu Zhang, and Nitesh V Chawla. Knowledge distillation on graphs: A survey. *arXiv preprint arXiv:2302.00219*, 2023.

Jan Tönshoff, Martin Ritzert, Eran Rosenbluth, and Martin Grohe. Where did the gap go? reassessing the long-range graph benchmark. *arXiv preprint arXiv:2309.00367*, 2023.

Anton Tsitsulin, John Palowitch, Bryan Perozzi, and Emmanuel Müller. Graph clustering with graph neural networks. *Journal of Machine Learning Research*, 24(127):1–21, 2023.

Aaron Van Den Oord, Oriol Vinyals, et al. Neural discrete representation learning. *Advances in neural information processing systems*, 30, 2017.

Petar Veličković, Guillem Cucurull, Arantxa Casanova, Adriana Romero, Pietro Liò, and Yoshua Bengio. Graph attention networks. In *International Conference on Learning Representations*, 2018a.

Petar Veličković, William Fedus, William L Hamilton, Pietro Liò, Yoshua Bengio, and R Devon Hjelm. Deep graph infomax. *arXiv preprint arXiv:1809.10341*, 2018b.

Clement Vignac, Igor Krawczuk, Antoine Siraudin, Bohan Wang, Volkan Cevher, and Pascal Frossard. Digress: Discrete denoising diffusion for graph generation. *arXiv preprint arXiv:2209.14734*, 2022.

Chun Wang, Shirui Pan, Ruiqi Hu, Guodong Long, Jing Jiang, and Chengqi Zhang. Attributed graph clustering: A deep attentional embedding approach. *arXiv preprint arXiv:1906.06532*, 2019a.

Kun Wang, Guohao Li, Shilong Wang, Guibin Zhang, Kai Wang, Yang You, Xiaojiang Peng, Yuxuan Liang, and Yang Wang. The snowflake hypothesis: Training deep gnn with one node one receptive field. *arXiv preprint arXiv:2308.10051*, 2023a.

Minjie Wang, Da Zheng, Zihao Ye, Quan Gan, Mufei Li, Xiang Song, Jinjing Zhou, Chao Ma, Lingfan Yu, Yu Gai, et al. Deep graph library: A graph-centric, highly-performant package for graph neural networks. *arXiv preprint arXiv:1909.01315*, 2019b.

Shuang Wang, Bahaeddin Eravci, Rustam Guliyev, and Hakan Ferhatosmanoglu. Low-bit quantization for deep graph neural networks with smoothness-aware message propagation. In *Proceedings of the 32nd ACM International Conference on Information and Knowledge Management*, pp. 2626–2636, 2023b.

Xiyuan Wang, Haotong Yang, and Muhan Zhang. Neural common neighbor with completion for link prediction. *arXiv preprint arXiv:2302.00890*, 2023c.

Qitian Wu, Wentao Zhao, Zenan Li, David P Wipf, and Junchi Yan. Nodeformer: A scalable graph structure learning transformer for node classification. *Advances in Neural Information Processing Systems*, 35:27387–27401, 2022.

Qitian Wu, Wentao Zhao, Chenxiao Yang, Hengrui Zhang, Fan Nie, Haitian Jiang, Yatao Bian, and Junchi Yan. Simplifying and empowering transformers for large-graph representations. In *Thirty-seventh Conference on Neural Information Processing Systems*, 2023. URL https://openreview.net/forum?id=R4xpvDTWkV.

Zhenqin Wu, Bharath Ramsundar, Evan N Feinberg, Joseph Gomes, Caleb Geniesse, Aneesh S Pappu, Karl Leswing, and Vijay Pande. Moleculenet: a benchmark for molecular machine learning. *Chemical science*, 9(2):513–530, 2018.

Jun Xia, Chengshuai Zhao, Bozhen Hu, Zhangyang Gao, Cheng Tan, Yue Liu, Siyuan Li, and Stan Z Li. Mole-bert: Rethinking pre-training graph neural networks for molecules. 2023.

Yan Xia, Hai Huang, Jieming Zhu, and Zhou Zhao. Achieving cross modal generalization with multimodal unified representation. *Advances in Neural Information Processing Systems*, 36, 2024.

Dongkuan Xu, Wei Cheng, Dongsheng Luo, Haifeng Chen, and Xiang Zhang. Infogcl: Information-aware graph contrastive learning. *Advances in Neural Information Processing Systems*, 34: 30414–30425, 2021.

Keyulu Xu, Weihua Hu, Jure Leskovec, and Stefanie Jegelka. How powerful are graph neural networks? *arXiv preprint arXiv:1810.00826*, 2018.

Bencheng Yan, Chaokun Wang, Gaoyang Guo, and Yunkai Lou. Tinygnn: Learning efficient graph neural networks. In *Proceedings of the 26th ACM SIGKDD International Conference on Knowledge Discovery & Data Mining*, pp. 1848–1856, 2020.

Chenxiao Yang, Qitian Wu, and Junchi Yan. Geometric knowledge distillation: Topology compression for graph neural networks. *Advances in Neural Information Processing Systems*, 35:29761–29775, 2022.

Ling Yang, Ye Tian, Minkai Xu, Zhongyi Liu, Shenda Hong, Wei Qu, Wentao Zhang, Bin CUI, Muhan Zhang, and Jure Leskovec. VQGraph: Rethinking graph representation space for bridging GNNs and MLPs. In *The Twelfth International Conference on Learning Representations*, 2024. URL https://openreview.net/forum?id=h6Tz85BqRI.

Zhilin Yang, William Cohen, and Ruslan Salakhudinov. Revisiting semi-supervised learning with graph embeddings. In *International conference on machine learning*, pp. 40–48. PMLR, 2016.

Ruosong Ye, Caiqi Zhang, Runhui Wang, Shuyuan Xu, and Yongfeng Zhang. Natural language is all a graph needs. *arXiv preprint arXiv:2308.07134*, 2023.

Yihang Yin, Qingzhong Wang, Siyu Huang, Haoyi Xiong, and Xiang Zhang. Autogcl: Automated graph contrastive learning via learnable view generators. In *Proceedings of the AAAI conference on artificial intelligence*, volume 36, pp. 8892–8900, 2022.

Chengxuan Ying, Tianle Cai, Shengjie Luo, Shuxin Zheng, Guolin Ke, Di He, Yanming Shen, and Tie-Yan Liu. Do transformers really perform badly for graph representation? *Advances in Neural Information Processing Systems*, 34:28877–28888, 2021.

Zhitao Ying, Jiaxuan You, Christopher Morris, Xiang Ren, Will Hamilton, and Jure Leskovec. Hierarchical graph representation learning with differentiable pooling. *Advances in neural information processing systems*, 31, 2018.

Yuning You, Tianlong Chen, Yongduo Sui, Ting Chen, Zhangyang Wang, and Yang Shen. Graph contrastive learning with augmentations. *Advances in neural information processing systems*, 33: 5812–5823, 2020.

Yuning You, Tianlong Chen, Yang Shen, and Zhangyang Wang. Graph contrastive learning automated. In *International Conference on Machine Learning*, pp. 12121–12132. PMLR, 2021.

Seongjun Yun, Seoyoon Kim, Junhyun Lee, Jaewoo Kang, and Hyunwoo J Kim. Neo-gnns: Neighborhood overlap-aware graph neural networks for link prediction. *Advances in Neural Information Processing Systems*, 34:13683–13694, 2021.

Bohang Zhang, Shengjie Luo, Liwei Wang, and Di He. Rethinking the expressive power of GNNs via graph biconnectivity. In *The Eleventh International Conference on Learning Representations*, 2023a. URL https://openreview.net/forum?id=r9hNv76KoT3.

Dalong Zhang, Xin Huang, Ziqi Liu, Zhiyang Hu, Xianzheng Song, Zhibang Ge, Zhiqiang Zhang, Lin Wang, Jun Zhou, Yang Shuang, et al. Agl: a scalable system for industrial-purpose graph machine learning. *arXiv preprint arXiv:2003.02454*, 2020.

Hengrui Zhang, Qitian Wu, Junchi Yan, David Wipf, and Philip S Yu. From canonical correlation analysis to self-supervised graph neural networks. *Advances in Neural Information Processing Systems*, 34:76–89, 2021a.

Muhan Zhang and Yixin Chen. Link prediction based on graph neural networks. *Advances in neural information processing systems*, 31, 2018.

Shichang Zhang, Yozen Liu, Yizhou Sun, and Neil Shah. Graph-less neural networks: Teaching old mlps new tricks via distillation. *arXiv preprint arXiv:2110.08727*, 2021b.

Shuai Zhang, Meng Wang, Pin-Yu Chen, Sijia Liu, Songtao Lu, and Miao Liu. Joint edge-model sparse learning is provably efficient for graph neural networks. In *The Eleventh International Conference on Learning Representations*, 2023b. URL https://openreview.net/forum?id=4UldFtZ_CVF.

Xiaotong Zhang, Han Liu, Qimai Li, and Xiao-Ming Wu. Attributed graph clustering via adaptive graph convolution. *arXiv preprint arXiv:1906.01210*, 2019.

Zaixi Zhang, Qi Liu, Hao Wang, Chengqiang Lu, and Chee-Kong Lee. Motif-based graph self-supervised learning for molecular property prediction. *Advances in Neural Information Processing Systems*, 34:15870–15882, 2021c.

Jianan Zhao, Le Zhuo, Yikang Shen, Meng Qu, Kai Liu, Michael Bronstein, Zhaocheng Zhu, and Jian Tang. Graphtext: Graph reasoning in text space. *arXiv preprint arXiv:2310.01089*, 2023.

Sipeng Zheng, Bohan Zhou, Yicheng Feng, Ye Wang, and Zongqing Lu. Unicode: Learning a unified codebook for multimodal large language models. *arXiv preprint arXiv:2403.09072*, 2024.

Zhaocheng Zhu, Zuobai Zhang, Louis-Pascal Xhonneux, and Jian Tang. Neural bellman-ford networks: A general graph neural network framework for link prediction. *Advances in Neural Information Processing Systems*, 34:29476–29490, 2021.

A SELF-SUPERVISED NODE IDS USING GRAPHCL

In this section, we discuss GraphCL (You et al., 2020) as a self-supervised learning (SSL) model for self-supervised Node IDs. Contrastive learning aims at learning an embedding space by comparing training samples and encouraging representations from positive pairs of examples to be close in the embedding space while representations from negative pairs are pushed away from each other. Such approaches usually consider each sample as its own class, that is, a positive pair consists of two different views of it; and all other samples in a batch are used as the negative pairs during training.

Specifically, a minibatch of N graphs is randomly sampled and subjected to contrastive learning. This process results in $2N$ augmented graphs, along with a corresponding contrastive loss to be optimized. We redefine $z_{n,i}$ and $z_{n,j}$ for the n-th graph in the minibatch. Negative pairs are not explicitly sampled but are instead generated from the other $N - 1$ augmented graphs within the same minibatch. The cosine similarity function is denoted as $\text{sim}(z_{n,i}, z_{n,j}) = \frac{z_{n,i}^T z_{n,j}}{\|z_{n,i}\|\|z_{n,j}\|}$. The NT-Xent loss (Sohn, 2016) for the n-th graph is then defined as:

$$\mathcal{L}_{\text{GraphCL}} = -\log \frac{\exp(\text{sim}(z_{n,i}, z_{n,j})/\tau)}{\sum_{n'=1, n' \neq n}^{N} \exp(\text{sim}(z_{n,i}, z_{n',j})/\tau)},$$

$$z_{n,i} = \text{R}\left(\text{MPNN}(v_{n,i}, A_{n,i}, X_{n,i})\right),$$

where τ represents the temperature parameter. The final loss is computed across all positive pairs in the minibatch. Consequently, Equation 7 is reformulated as:

$$\mathcal{L}_{\text{NID}} = \mathcal{L}_{\text{GraphCL}} + \sum_{n \in [1,N]} \sum_{v_{n,i} \in \mathcal{V}_{n,i}} \mathcal{L}_{\text{VQ}}(v_{n,i}) + \sum_{v_{n,j} \in \mathcal{V}_{n,j}} \mathcal{L}_{\text{VQ}}(v_{n,j}), \tag{14}$$

B PROOF OF THEOREM 1

Proof. For node $v \in \mathcal{V}$ with label $p \in \{0, 1, \cdots, P - 1\}$, by data formulation in Section 3.3, we have that there exists at least one node $u \in \mathcal{N}(v)$ that satisfies $x_u = \mu_p$. Given (7), let the first-round clustering center for v be $c_v = c_v^{\parallel} + c_v^{\perp}$, where $c_v^{\parallel}$ is in the direction of $W\mu_p$ and $c_v^{\perp} \perp W\mu_p$. By the assumption on W, we know that $W\mu_i \perp W\mu_j$ if $i \neq j$, $i, j \in [P]$, and $W\mu_i = 0$ for $i > P$. Therefore,

$$\|\frac{1}{|\mathcal{N}(v)|} \sum_{u \in \mathcal{N}_v} W x_u - c_v\|^2$$
$$= \|\frac{1}{|\mathcal{N}(v)|} \sum_{u \in \mathcal{N}_v, x_u = \mu_p} W x_u - c_v^{\parallel}\|^2 + \|\frac{1}{|\mathcal{N}(v)|} \sum_{u \in \mathcal{N}_v, x_u \neq \mu_p} W x_u - c_v^{\perp}\|^2. \tag{15}$$

Note that there is no node $u \in \mathcal{N}(v)$ such that $x_u = \mu_j$ for $j \neq p$ and $j \in [P]$. Therefore, we can show that the optimized $c_v^{\parallel}$ by (7) is in the direction of $W\mu_p$, and

$$\|c_v^{\parallel}\| \geq \frac{1}{D_{\mathcal{G}}}, \tag{16}$$

since that

$$\frac{1}{|\mathcal{N}(v)|} \sum_{u \in \mathcal{N}_v} \mathbb{1}[x_u = \mu_p] \geq \frac{1}{D_{\mathcal{G}}}. \tag{17}$$

Hence, we can obtain that the optimized clustering center c_{v_1} and c_{v_2} for $v_1, v_2 \in \mathcal{V}$ with $y_{v_1} \neq y_{v_2}$, we have

$$\|c_{v_1} - c_{v_2}\| \geq \frac{\sqrt{2}}{D_{\mathcal{G}}} \geq \Omega(1), \tag{18}$$

which means that c_{v_1} and c_{v_1} are distinct enough given $D_{\mathcal{G}} \leq O(1)$. Then, we have

$$\text{Node\_ID}(v_1) \neq \text{Node\_ID}(v_2). \tag{19}$$

Then, we analyze the learning process with a linear layer. Let $\boldsymbol{V} = (\boldsymbol{v}_1, \boldsymbol{v}_2, \cdots, \boldsymbol{v}_P)$. The gradient of the loss function against $\boldsymbol{v}_j$, $j \in [P]$, is computed as

$$
\begin{aligned}
&\frac{1}{|\mathcal{V}_R|} \sum_{v \in \mathcal{V}_R} \frac{\partial \ell(\boldsymbol{z}_v, y_v; \boldsymbol{V})}{\partial \boldsymbol{v}_j} \\
=&\frac{1}{|\mathcal{V}_R|} \sum_{v \in \mathcal{V}_R, y_v = j} -\frac{1}{\hat{p}_{v,j}} \hat{p}_{v,j}(1 - \hat{p}_{v,j})\boldsymbol{z}_v + \frac{1}{|\mathcal{V}_R|} \sum_{v \in \mathcal{V}_R, y_v = j' \neq j} -\frac{1}{\hat{p}_{v,j}}(-\hat{p}_{v,j}\hat{p}_{v,j'})\boldsymbol{z}_v \\
=&\frac{1}{|\mathcal{V}_R|} \sum_{v \in \mathcal{V}_R, y_v = j} (\hat{p}_{v,j} - 1)\boldsymbol{z}_v + \frac{1}{|\mathcal{V}_R|} \sum_{v \in \mathcal{V}_R, y_v = j' \neq j} \hat{p}_{v,j'}\boldsymbol{z}_v.
\end{aligned} \tag{20}
$$

Note that $\hat{p}_{v,j} - 1 < 0$, $\hat{p}_{v,j'} > 0$. At iteration 0, $\boldsymbol{V}$ follows a Gaussian distribution and is close to 0, which makes the distribution of $\{\hat{p}_{v,i}\}_{i=1}^P$ close to be uniform. Therefore, after T iterations, we have that

$$
\boldsymbol{v}_j^{(T)} = \boldsymbol{v}_j^{(0)} + \frac{\eta}{|\mathcal{V}_R|} \sum_{v \in \mathcal{V}_R, y_v = j} (1 - \hat{p}_{v,j})\boldsymbol{z}_v - \frac{\eta}{|\mathcal{V}_R|} \sum_{v \in \mathcal{V}_R, y_v = j' \neq j} \hat{p}_{v,j'}\boldsymbol{z}_v, \tag{21}
$$

where $\eta \leq O(1)$ is the step size. We know that for all the nodes $v \in \mathcal{V}_R$ with $y_v = j$, the first d_e dimensions are the same. Denote the first d_e dimensions of $\boldsymbol{v}_j^{(T)}$ as $\boldsymbol{v}_{j,1:d_e}^{(T)}$. Then, after $T = \Omega(\eta^{-1}P)$ iterations, the magnitude of $\boldsymbol{v}_{j,1:d_e}^{(T)}$ in the direction of the embedding of the first digit of Node_ID(v) is

$$
\Omega(\eta^{-1}P) \cdot \frac{\eta}{\mathcal{V}_R} \sum_{v \in \mathcal{V}_R} \mathbb{1}[y_v = j] \geq \Omega(1). \tag{22}
$$

Moreover, the magnitude of $\boldsymbol{v}_{j,1:d_e}^{(T)}$ in the direction of the embedding of other digit of Node_ID(v) is

$$
-\Omega(\eta^{-1}P) \cdot \frac{\eta}{\mathcal{V}_R} \sum_{v \in \mathcal{V}_R} \mathbb{1}[y_v = j' \neq j] \cdot \frac{1}{P} \leq -\Omega(\frac{1}{P}). \tag{23}
$$

Note that the probability of a d_e-dimensional embedding for other digits other than the first one is $O(1/K)$. Hence, by $r < K$, we can ensure that the first d_e dimensions are the dominant part for prediction. Therefore, for a given $\boldsymbol{z}_v$ for $v \in \mathcal{G}$, $y_v = j$, we have

$$
\boldsymbol{z}_v^\top \boldsymbol{v}_j^{(T)} - \boldsymbol{z}_v^\top \boldsymbol{v}_{j'}^{(T)} \geq \Omega(1), \tag{24}
$$

so that

$$
\hat{p}_{v,j} > \hat{p}_{v,j'}. \tag{25}
$$

We can then derive that for any $v \in \mathcal{V}$,

$$
\mathbb{1}[y_v \neq \arg \max_{i \in [P]} \hat{\boldsymbol{p}}_{v,i}] = 0. \tag{26}
$$

$\square$

C   DATASETS AND EXPERIMENTAL DETAILS

C.1   COMPUTING ENVIRONMENT

Our implementation is based on PyG (Fey & Lenssen, 2019) and DGL (Wang et al., 2019b). The experiments are conducted on a single workstation with 8 RTX 3090 GPUs.

C.2   DESCRIPTION OF DATASETS

Table 11 presents a summary of the statistics and characteristics of the datasets. The initial eight datasets are sourced from TUDataset (Morris et al., 2020), followed by two from LRGB (Dwivedi et al., 2022), and finally the remaining datasets are obtained from Hu et al. (2020); Kipf & Welling (2017); Chien et al. (2020); Pei et al. (2019); Rozemberczki et al. (2021); McAuley et al. (2015); Leskovec & Krevl (2016); Mernyei & Cangea (2020); Lim et al. (2021); Platonov et al. (2023).

Table 11: Overview of the graph learning dataset used in this work (Morris et al., 2020; Dwivedi et al., 2022; Kipf & Welling, 2017; Chien et al., 2020; Pei et al., 2019; Rozemberczki et al., 2021; Hu et al., 2020; McAuley et al., 2015; Leskovec & Krevl, 2016; Mernyei & Cangea, 2020; Lim et al., 2021; Platonov et al., 2023).

Dataset	# Graphs	Avg. # nodes	Avg. # edges	# Feats	Prediction level	Prediction task	Metric
Cora	1	2,708	5,278	2,708	node	7-class classif.	Accuracy
Citeseer	1	3,327	4,522	3,703	node	6-class classif.	Accuracy
Pubmed	1	19,717	44,324	500	node	3-class classif.	Accuracy
Computer	1	13,752	245,861	767	node	10-class classif.	Accuracy
Photo	1	7,650	119,081	745	node	8-class classif.	Accuracy
CS	1	18,333	81,894	6,805	node	15-class classif.	Accuracy
Physics	1	34,493	247,962	8,415	node	5-class classif.	Accuracy
WikiCS	1	11,701	216,123	300	node	10-class classif.	Accuracy
Squirrel	1	2,223	46,998	2,089	node	5-class classif.	Accuracy
Chameleon	1	890	8,854	2,325	node	5-class classif.	Accuracy
Amazon-ratings	1	24,492	93,050	300	node	5-class classif.	Accuracy
Questions	1	48,921	153,540	301	node	2-class classif.	ROC-AUC
ogbn-arxiv	1	169,343	1,166,243	128	node	40-class classif.	Accuracy
ogbn-proteins	1	132,534	39,561,252	8	node	112 binary classif.	ROC-AUC
ogbn-products	1	2,449,029	61,859,140	100	node	47-class classif.	Accuracy
pokec	1	1,632,803	30,622,564	65	node	binary classif.	Accuracy
ogbl-collab	1	235,868	1,285,465	128	edge	link prediction	Hits@50
Peptides-func	15,535	150.9	307.3	9	graph	10-task classif.	AP
Peptides-struct	15,535	150.9	307.3	9	graph	11-task regression	MAE
NCI1	4,110	29.87	32.30	37	graph	2-class classif.	Accuracy
MUTAG	188	17.93	19.79	7	graph	2-class classif.	Accuracy
PROTEINS	1,113	39.06	72.82	3	graph	2-class classif.	Accuracy
DD	1,178	284.32	715.66	89	graph	2-class classif.	Accuracy
COLLAB	5,000	74.49	2457.78	1	graph	3-class classif.	Accuracy
REDDIT-BINARY	2,000	429.63	497.75	1	graph	2-class classif.	Accuracy
REDDIT-MULTI-5K	4,999	508.52	594.87	1	graph	5-class classif.	Accuracy
IMDB-BINARY	1,000	19.77	96.53	1	graph	2-class classif.	Accuracy

- Supervised Node Classification: Cora, Citeseer, Pubmed, Computer, Photo, CS, Physics, WikiCS, Amazon-ratings, Questions, Squirrel, Chameleon, ogbn-arxiv, ogbn-proteins, ogbn-products and pokec. For Cora, Citeseer, and Pubmed, we employ a training/validation/testing split ratio of 60%/20%/20% and use accuracy as the evaluation metric, consistent with Pei et al. (2019). For Squirrel, Chameleon, Amazon-ratings and Questions, we adhere to the standard splits and evaluation metrics outlined in Platonov et al. (2023). For the remaining datasets, standard splits and metrics are followed as specified in Luo et al. (2024b). For comprehensive details on these datasets, please refer to the respective studies (Pei et al., 2019; Luo et al., 2024b).

- Supervised Link Prediction: Cora, Citeseer, Pubmed, ogbl-collab. We follow the standard splits and evaluation metrics specified in Wang et al. (2023c), with further details provided therein.

- Supervised Graph Classification: Peptides-func and Peptides-struct. For each dataset, we follow the standard train/validation/test splits and evaluation metrics in Rampášek et al. (2022). For more comprehensive details, readers are encouraged to refer to Rampášek et al. (2022).

- Attributed Graph Clustering: Cora, Citeseer, PubMed, Computer, Photo, Physics, ogbn-arxiv. To evaluate the clustering performance, we adopt two performance measures: NMI and F1, following the approach used in DGCluster (Bhowmick et al., 2024).

- Unsupervised Node Classification: Cora, Citeseer, Pubmed. For each dataset, we follow the standard splits and evaluation metrics in GraphMAE (Hou et al., 2022).

- Unsupervised Graph Classification: NCI1, PROTEINS, DD, MUTAG, COLLAB, REDDIT-B, REDDIT-M5K, and IMDB-B. Each dataset is a collection of graphs where each graph is associated with a label. Each dataset consists of a set of graphs, with each graph associated with a label. For NCI1, PROTEINS, DD, and MUTAG, node labels serve as input features, while for COLLAB, REDDIT-B, REDDIT-M5K, and IMDB-B, node degrees are utilized. In each dataset, we follow exactly the same data splits and evaluation metircs as the standard settings (You et al., 2020).

C.3 BASELINES

Attributed Graph Clustering. We apply baseline methods from DGCluster (Bhowmick et al., 2024): SBM (Peixoto, 2014), AGC Zhang et al. (2019), SDCN (Bo et al., 2020), DAEGC (Wang et al., 2019a), NOCD (Shchur & Günnemann, 2019), DiffPool (Ying et al., 2018), MinCut (Bianchi et al., 2020), Ortho (Bianchi et al., 2020), DMoN (Tsitsulin et al., 2023) and DGCluster (Bhowmick et al., 2024).

Unsupervised Node Classification. We utilize all the baselines from GraphMAE (Hou et al., 2022): GAE (Kipf & Welling, 2016), DGI (Veličković et al., 2018b), MVGRL (Hassani & Khasahmadi, 2020), InfoGCL (Xu et al., 2021), CCA-SSG(Zhang et al., 2021a) and GraphMAE (Hou et al., 2022).

Unsupervised Graph Classification. We utilize the baselines from GraphCL (You et al., 2020) and AutoGCL (Yin et al., 2022): InfoGraph (Sun et al., 2019), MVGRL (Hassani & Khasahmadi, 2020), GraphCL (You et al., 2020), JOAO (You et al., 2021), GraphMAE (Hou et al., 2022), AD-GCL Suresh et al. (2021) and AutoGCL (Yin et al., 2022).

Supervised Node Classification. We compare our method to the following prevalent GNNs and transformer models from Polynormer (Deng et al., 2024): GCN (Kipf & Welling, 2017), SAGE (Hamilton et al., 2017), GAT (Veličković et al., 2018a), APPNP (Gasteiger et al., 2018), GPRGNN (Chien et al., 2020), LINKX (Lim et al., 2021), Polynormer (Deng et al., 2024), SGFormer (Wu et al., 2023). Furthermore, various other GTs like (Kong et al., 2023; Wu et al., 2022; Chen et al., 2022b; Rampášek et al., 2022; Shirzad et al., 2023; Dwivedi et al., 2023; Liu et al., 2023; Zhang et al., 2023a; Kuang et al., 2021; Luo et al., 2024a; Bo et al., 2023; Chen et al., 2022a; Ying et al., 2021; Dwivedi & Bresson, 2020) exist in related surveys (Hoang et al., 2024; Müller et al., 2023), empirically shown to be inferior to the GTs we compared against for node classification tasks.

Supervised Link Prediction. We employ all the baselines from NCN (Wang et al., 2023c): GCN (Kipf & Welling, 2017), SEAL (Zhang & Chen, 2018), NBFnet (Zhu et al., 2021), Neo-GNN (Yun et al., 2021), BUDDY (Chamberlain et al., 2022), NCN (Wang et al., 2023c).

Supervised Graph Classification. We compare our method to the GCN (Kipf & Welling, 2017). In terms of transformer models, we consider GT(Dwivedi & Bresson, 2020), Graph ViT (He et al., 2023), Exphormer (Shirzad et al., 2023), GraphGPS (Rampášek et al., 2022), and GRIT (Ma et al., 2023).

We report the performance of baseline models using results from their original papers or official leaderboards, where available, as these are derived from well-tuned configurations. For baselines without publicly available results on specific datasets, we tune their hyperparameters within our search space and tune their unique hyperparameters (not present in MPNNs) according to the search space specified in their original papers to attain the best possible results.

C.4 HYPERPARAMETERS AND REPRODUCIBILITY

Our source code is available at https://github.com/LUOyk1999/NodeID.

RVQ Implementation Details. As outlined in Sec. 3.1, RVQ is used to quantize the MPNN multi-layer embeddings of a node. The selection of MPNNs and the number of layers L are tailored to distinct datasets. For the embeddings from each layer, a consistent three-level ($M = 3$) residual quantization is implemented. And cosine similarity serves as the distance metric $|| \cdot ||$ within the RVQ framework. The codebook size K is tuned in $\{4, 6, 8, 16, 32\}$. The β is set to 1.

For the hyperparameter selections of our NID framework, in addition to what we have covered, we list other settings in Table 12. The tasks are presented in the following order: attributed graph clustering, unsupervised node classification, unsupervised graph classification, supervised node classification, supervised link prediction, and supervised graph classification. Below we detail the experimental settings for pretraining the node ID.

Attributed Graph Clustering. We implement our NID on top of the GCN in DGCluster (Bhowmick et al., 2024). To ensure a fair comparison, we use the same hyperparameters, including the number of layers, learning rate, hidden dimensions, and clustering method, as in DGCluster (Bhowmick et al., 2024).

Table 12: Task-specific hyperparameter settings of NID framework. The tasks are presented in the following order: attributed graph clustering, unsupervised node classification, unsupervised graph classification, supervised node classification, supervised link prediction, and supervised graph classification.

Dataset	Codebook size K	MPNN	MPNNs layer L	Hidden dim	LR	epoch	MLP layer
Cora	6	GCN	3	256	0.001	300	-
Citeseer	6	GCN	3	256	0.001	300	-
Pubmed	6	GCN	3	256	0.001	300	-
Computer	6	GCN	3	256	0.001	300	-
Photo	6	GCN	3	256	0.001	300	-
Physics	6	GCN	3	256	0.001	300	-
ogbn-arxiv	6	GCN	5	256	0.001	300	-
Cora	32	GCN	2	1024	0.001	1500	3
Citeseer	8	GCN	2	256	0.001	500	3
Pubmed	16	GCN	2	128	0.0005	500	3
NCI1	4	GIN	5	32	0.01	20	-
MUTAG	16	GIN	4	32	0.01	20	-
PROTEINS	8	GIN	3	32	0.01	20	-
DD	4	GIN	4	32	0.01	20	-
COLLAB	32	GIN	5	32	0.01	20	-
REDDIT-BINARY	4	GIN	5	32	0.01	20	-
REDDIT-MULTI-5K	4	GIN	4	32	0.01	20	-
IMDB-BINARY	8	GIN	3	32	0.01	20	-
Cora	6	GCN	4	128	0.01	1000	5
Citeseer	8	GCN	2	128	0.01	1000	5
Pubmed	16	GCN	2	256	0.005	1000	5
Computer	8	GAT	6	512	0.001	1200	5
Photo	4	GAT	6	512	0.001	1200	4
CS	16	GAT	7	512	0.001	1600	4
Physics	4	GAT	5	512	0.001	1600	4
WikiCS	8	GAT	8	512	0.001	1000	4
Squirrel	8	GCN	6	64	0.005	1000	2
Chameleon	32	GCN	3	256	0.005	1000	2
Amazon-ratings	16	GAT	12	512	0.001	2500	4
Questions	4	GAT	5	512	0.00003	1500	4
ogbn-arxiv	16	SAGE	5	256	0.0005	1000	4
ogbn-proteins	4	SAGE	4	256	0.0005	1000	5
ogbn-products	16	SAGE	5	128	0.003	1000	4
pokec	16	SAGE	7	256	0.0005	2000	5
Cora	32	GCN	10	256	0.004	150	3
Citeseer	8	GCN	10	256	0.01	10	3
Pubmed	8	GCN	10	256	0.01	100	3
ogbl-collab	16	GCN	5	256	0.001	150	3
Peptides-func	16	GCN	6	235	0.001	500	5
Peptides-struct	16	GCN	6	235	0.001	250	5

Unsupervised Node Classification. The pretraining hyperparameters are selected within the Graph-MAE's grid search space, as outlined in Table 12. All other experimental parameters, including dropout, batch size, training schemes, and optimizer, etc., align with those used in GraphMAE (Hou et al., 2022).

Unsupervised Graph Classification. Similarly, our pretraining hyperparameters in table are determined within GraphCL's grid search space. All other experimental parameters match those used in GraphCL (You et al., 2020). Specially for this task, following GraphCL (You et al., 2020), we input $\mathbf{NID}_{\mathrm{CL}}$ codes into a downstream LIBSVM (Chang & Lin, 2011) classifier. And models are trained for 20 epochs and tested every 10 epochs. We conduct a 10-fold cross-validation on every dataset. For each fold, we utilize 90% of the total data as the unlabeled data and the remaining 10% as the labeled testing data. Every experiment is repeated 5 times using different random seeds, with mean and standard deviation of accuracies (%) reported.

Supervised Node Classification. The pretraining hyperparameters listed in the table are based on the grid search space from Luo et al. (2024b). All other experimental parameters follow those outlined in the same study.

Supervised Link Prediction. Our pretraining hyperparameters in table are chosen from the NCN's grid search space. All other experimental parameters match those used in NCN (Wang et al., 2023c). For the Cora, CiteSeer, and PubMed datasets, we employ the Hadamard product as the readout

function. For ogbl-collab, we use *sum* pooling on the node IDs of the 1-hop common neighbors (Wang et al., 2023c; Barabási & Albert, 1999) to nodes u and v for the edge (u, v).

Supervised Graph Classification. All experimental parameters are consistent with those used by Tönshoff et al. (2023); Luo et al. (2025a).

Applications of Node IDs for Graph Learning. After obtaining the ID, we train the Multi-Layer Perceptron (MLP) for different tasks, with the number of layers specified in Table 12 and hidden dimensions of either 256 or 512. We utilize the Adam optimizer (Kingma & Ba, 2014) with the default settings. We set a learning rate of either 0.01 or 0.001 and an epoch limit of 1000. The ReLU function serves as the non-linear activation. Further details regarding hyperparameters can be found in the code in the supplementary material. In all experiments, we use the validation set to select the best hyperparameters. All results are derived from 10 independent runs, with mean and standard deviation of results reported.

D ADDITIONAL RESULTS
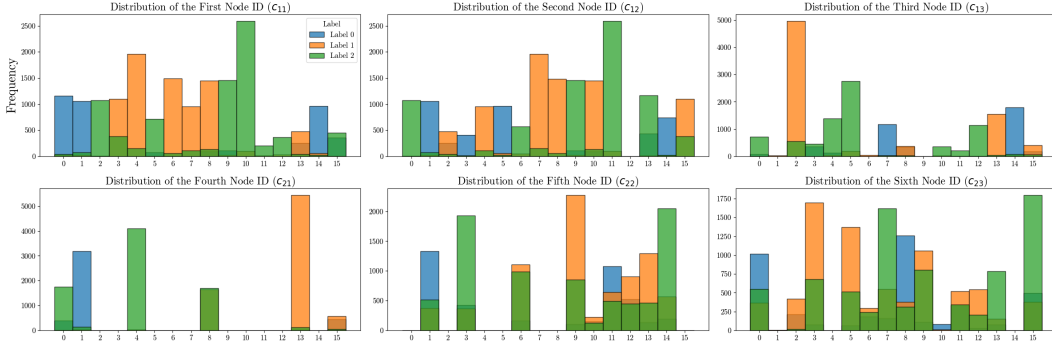
D.1 QUALITATIVE ANALYSIS

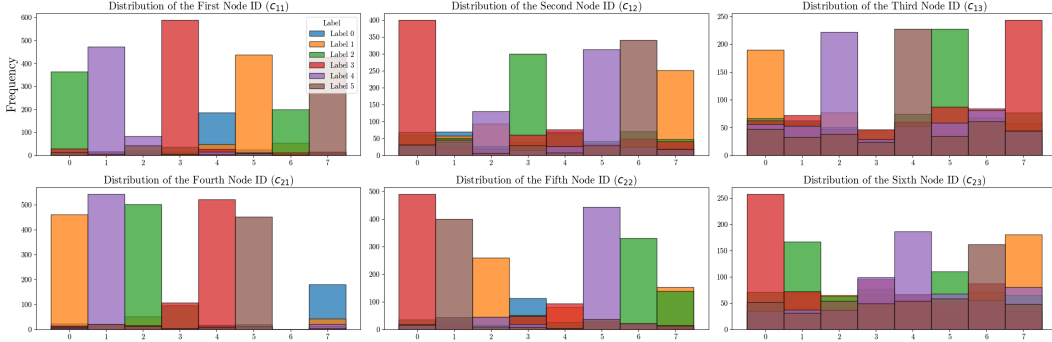Figure 7: The codeword distributions of the node IDs in PubMed colored by the ground-truth labels.

Figure 8: The codeword distributions of the node IDs in CiteSeer colored by the ground-truth labels.

D.2 ADDITIONAL LINEAR PROBING

Datasets. To evaluate the transferability of the proposed method, we test the performance through linear probing on molecular property prediction, adhering to the settings described by You et al. (2020). Initially, the NID_{CL} is pre-trained on 2 million unlabeled molecules sourced from ZINC15 (Hu* et al., 2020).

- Node features:
  - Atom number: $[1, 118]$
  - Chirality tag: {unspecified, tetrahedral cw, tetrahedral ccw, other}
- Edge features:
  - Bond type: {single, double, triple, aromatic}
  - Bond direction: {–, endupright, enddownright}

Then, we focus on molecular property prediction, where we adopt the widely-used 7 binary classification datasets contained in MoleculeNet (Wu et al., 2018) for linear probing. The scaffold-split (Ramsundar et al., 2019) is used to split downstream dataset graphs into training/validation/testing set as 80%/10%/10% which mimics real-world use cases. For the evaluation protocol, we run experiments for 10 times and report the mean and standard deviation of ROC-AUC scores (%).

Model Hyperparameters. Following You et al. (2020), we adopt a 5-layer GIN (Xu et al., 2018) with a 300 hidden dimension as the MPNN architecture, and set the RVQ codebook size at $K = 16$. We use mean pooling as the readout function. During the pre-training stage, GIN is pre-trained for 100 epochs with batch-size as 256 and the learning rate as 0.001. After the model is trained on the pre-training dataset, it is directly applied to the downstream dataset to obtain node IDs. To evaluate the learned node IDs, we follow the linear probing (linear evaluation) (Akhondzadeh et al., 2023), where a linear classifier (1 linear layer) is trained on the node IDs. During the probing stage, we train for 100 epochs with batch-size as 32, dropout rate as 0.5, and report the test performance using ROC-AUC at the best validation epoch.

The results are presented in Table 13. It is noteworthy that NID_{CL} outperforms the baselines in the SIDER, ClinTox, and BBBP datasets, and shows significant improvement over the embeddings from GraphCL. This suggests the robust transferability of NID_{CL}.

Table 13: Linear probing: molecular property prediction; binary classification, ROC-AUC (%).

	Tox21	ToxCast	Sider	ClinTox	HIV	BBBP	Bace
EdgePred	62.7 ± 0.6	55.3 ± 0.4	51.0 ± 0.3	48.9 ± 6.5	64.9 ± 2.0	54.8 ± 0.7	68.8 ± 0.9
ContextPred	68.4 ± 0.3	59.1 ± 0.2	59.4 ± 0.3	43.2 ± 1.7	68.9 ± 0.4	59.1 ± 0.2	64.4 ± 0.6
AttrMask	69.1 ± 0.2	58.2 ± 0.2	51.7 ± 0.1	51.6 ± 0.7	60.9 ± 1.3	61.0 ± 1.3	64.4 ± 2.5
JOAO	70.6 ± 0.4	60.5 ± 0.3	57.4 ± 0.6	54.1 ± 2.6	68.1 ± 0.9	63.7 ± 0.3	71.2 ± 1.0
SimGRACE	64.6 ± 0.4	59.1 ± 0.2	54.9 ± 0.6	63.4 ± 2.6	66.3 ± 1.5	65.4 ± 1.2	67.8 ± 1.3
GraphCL	64.4 ± 0.5	59.4 ± 0.2	54.6 ± 0.3	59.8 ± 1.2	63.7 ± 2.3	62.4 ± 0.7	71.1 ± 0.7
NID_{CL}	66.3 ± 0.4	59.1 ± 0.3	**60.1 ± 0.4**	**65.3 ± 2.2**	64.3 ± 0.8	**66.9 ± 0.6**	66.1 ± 1.2

D.3 ADDITIONAL COMPARISON RESULTS WITH VQGRAPH

Efficiency. Our NID employs RVQ at every layer of the MPNN, achieving a representational capacity of $O(K^{M^L})$ with only $O(K \times M \times L)$ in codebook size, which far surpasses VQGraph's capacity that is limited to its single codebook size. As depicted in Table 14, NID_{GCN} is considerably more efficient than VQGraph.

Quality. We specifically compare the node classification results with VQGraph tokens under the same experimental settings. VQGraph tokens refers to training an MLP with tokens learned by VQGraph tokenizer from Yang et al. (2024). As shown in Table 15, VQGraph tokens lack structural information, likely due to codebook collapse encountered by their tokenizer (see Table 8).

Table 14: Comparison of optimal total codebook sizes.

	Cora	CiteSeer	PubMed	Computer
VQGraph	2048	4096	8192	16384
NID_{GCN} ($K \times M \times L$)	$6 \times 3 \times 4 = 72$	$8 \times 3 \times 2 = 48$	$16 \times 3 \times 2 = 96$	$8 \times 3 \times 5 = 120$

Table 15: Node classification results in supervised representation learning.

Metric	Cora Accuracy↑	CiteSeer Accuracy↑	PubMed Accuracy↑	ogbn-arxiv Accuracy↑
VQGraph tokens	63.39 ± 1.15	32.07 ± 2.70	54.37 ± 4.76	43.57 ± 0.49
NID_{GCN}	87.88 ± 0.69	76.89 ± 1.09	89.42 ± 0.44	71.27 ± 0.24

D.4 HIGH CODEBOOK USAGE IN NID

In response to the surprising high codebook usage of our NID compared to VQGraph, we believe this is primarily due to our small codebook size K.

As detailed in Table 14, NID achieves high codebook utilization without experiencing codebook collapse. This efficiency is attributed to our smaller codebook size K, typically less than 32. In contrast, VQGraph uses a significantly larger codebook size, ranging from 2048 to 32,768 (as reported in Table 12 of the VQGraph paper (Yang et al., 2024)). Their codebook size typically scales the graph size; for example, on the Citeseer dataset, which comprises 2,110 nodes, they used a codebook size of 4,096.

We have observed that a large codebook size often leads to severe codebook collapse. Our use of a small codebook size ensures high codebook usage and prevents codebook collapse. These observations are consistent with findings reported in FSQ (Mentzer et al., 2024).

D.5 RECONSTRUCTION TASK EXCLUSION IN $\mathcal{L}_{\text{NID}}$

In this section, we address the exclusion of the reconstruction task in our $\mathcal{L}_{\text{NID}}$, differentiating it from other methods such as VQ-VAE and VQGraph. A reconstruction task typically involves using code vectors to regenerate the input data, aiming to minimize the difference between the original input and its reconstruction.

Our decision to omit a reconstruction loss component was based on an ablation study comparing our approach with VQGraph. By replicating VQGraph's experimental setup, minus the reconstruction loss, we found that omitting this component had a negligible impact on performance, as shown in Table 16.

Moreover, as suggested by Vignac et al. (2022), generative models like VQ-VAE, which are primarily designed for continuous data, encounter challenges with graph data due to difficulties in preserving the sparsity and discrete structure inherent in graphs. Therefore, our approach simplifies the model by not involve using the code vectors for a reconstruction task.

Table 16: Impact of excluding reconstruction loss on performance

Model	Cora	CiteSeer	PubMed	ogbn-products
VQGraph	76.08 ± 0.55	78.40 ± 1.71	83.93 ± 0.87	79.17 ± 0.21
VQGraph without reconstruction loss	76.17 ± 0.47	78.03 ± 1.58	83.85 ± 1.24	79.23 ± 0.26

D.6 END-TO-END LEARNING WITH RVQ

RVQ can feasibly be applied post-hoc to embeddings generated by a GNN. However, this approach requires a two-phase training process: initially training the GNN and subsequently training the RVQ model. Each phase demands separate optimization of parameters, such as learning rates and epochs.

We conducted experiments to evaluate both methods: end-to-end learning versus post-hoc RVQ application. The results, summarized in Table 17, illustrate that end-to-end learning not only streamlines the training process but also improves performance.

Table 17: Comparison of end-to-end and post-hoc RVQ learning performance

Method	Cora	Citeseer	PubMed
$\mathbf{NID}_{\text{GCN}}$ (End-to-End Learning)	87.88 ± 0.69	76.89 ± 1.09	89.42 ± 0.44
$\mathbf{NID}_{\text{GCN}}$ (Post-hoc RVQ)	86.17 ± 0.33	75.47 ± 1.31	88.32 ± 0.54

D.7 TRANSDUCTIVE VS. INDUCTIVE INFERENCE

It is important to clarify that our manuscript also incorporates inductive inference evaluations. Notably, the experiments documented in Table 3 & 4 involve inductive graph and edge inference.

For instance, in the Peptides-func dataset detailed in Table 3, we classified 15,535 graphs that were split into training, validation, and test sets. The key point here is that the graphs used during the inference stage were not exposed to the model during training. Additionally, we followed the inductive settings described in the VQGraph paper (Yang et al., 2024) to perform node classification experiments on the ogbn-products dataset. The results in Table 18 clearly demonstrate that our NID method achieves superior performance in both inductive and transductive settings.

Table 18: Comparison of inductive and transductive inference performance on ogbn-products

Model	ogbn-products (Inductive)	ogbn-products (Transductive)
VQGraph	77.50 ± 0.25	79.17 ± 0.21
$\mathbf{NID}_{\text{SAGE}}$	79.13 ± 0.32	81.83 ± 0.26

E ADDITIONAL DISCUSSION

E.1 RVQ IMPLEMENTATION DETAILS

In our model, each MPNN layer involves the use of M codewords per node, which implies that RVQ is conducted over M iterations.

It is crucial to note that for each MPNN layer, an independent set of M codebooks is utilized. Specifically, we quantize the node embedding $\boldsymbol{h}_v^l$ by sequentially selecting the closest code vector from each codebook:

- The first code vector $\boldsymbol{e}_{c_{l1}}$ (c_{l1} is the codeword) is chosen based on the initial node embedding $\boldsymbol{r}_{l1} = \boldsymbol{h}_v^l$.
- Subsequent code vectors, such as $\boldsymbol{e}_{c_{l2}}$, are selected based on the residual vector $\boldsymbol{r}_{l2} = \boldsymbol{h}_v^l - \boldsymbol{r}_{l1}$, and so forth.

For each codebook approximation, we optimize two types of losses: the codebook loss and the commitment loss, as detailed in Equation 8. Taking the $\mathbf{NID}_{\text{MAE}}$ as an example, during training, we aggregate all losses from each codebook across all layers ($L \times M$) into an additional loss component. This component is then jointly optimized with the MAE loss, as described in Equation 9, within a single backpropagation step.

E.2 PRETRAINING RUNTIME

One pertinent aspect of our paper involves analyzing the computational complexity associated with the multi-level optimization of codebooks. To elucidate this, we compared the training time per epoch of our $\mathbf{NID}_{\text{SAGE}}$ with SAGE on ogbn-products, ogbn-proteins and pokec (see Table 19). The results are revealing: the NID model records a training time of 5.9 seconds per epoch, closely mirroring

that of SAGE, which is at 5.8 seconds per epoch. This comparison substantiates that the additional quantization module integrated into our NID model imposes minimal computational overhead.

These findings underscore the efficiency of our NID model, demonstrating its capability to maintain comparable training times to traditional GNNs despite the added complexity of the multi-level codebook optimization.

Table 19: Empirical training runtime per epoch on ogbn-proteins, ogbn-products, and pokec.

Dataset	# Nodes	# Edges	Training Time per Epoch
ogbn-proteins	132,534	39,561,252	SAGE: 0.45s, NID_{SAGE}: 0.51s
ogbn-products	2,449,029	61,859,140	SAGE: 5.8s, NID_{SAGE}: 5.9s
pokec	1,632,803	30,622,564	SAGE: 2.7s, NID_{SAGE}: 3.1s

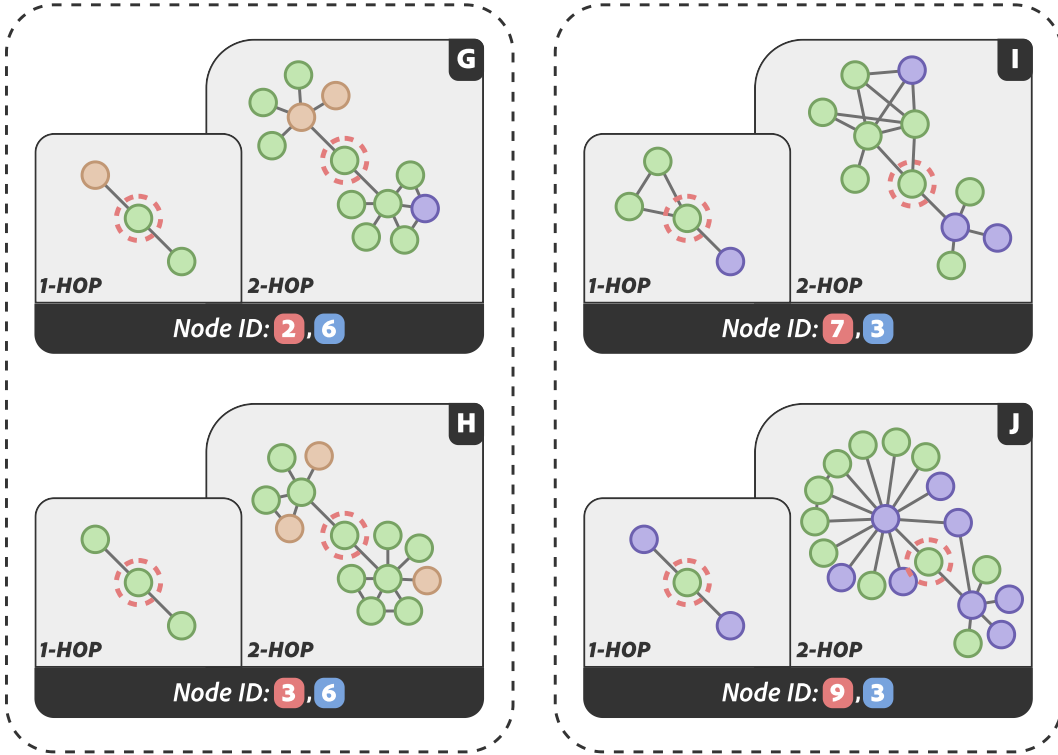### E.3 EXAMPLES OF NODE IDS WITH THE SAME SECOND ID CODE

Figure 9: Two real examples of node IDs with the same second ID code from Figure 1 in the PubMed dataset. Nodes G and H have different first ID codes because, despite sharing a similar 1-hop topology, they differ in the label distribution of their 1-hop neighbors. However, they exhibit a similar 2-hop topology and similar label distributions among their 2-hop neighbors, which results in the same second ID code. Additionally, nodes I and J have different first ID codes due to differences in both their 1-hop topologies and the label distributions among their 1-hop neighbors. Nevertheless, their 2-hop neighbors share similar label distributions, leading to the same second ID code, even though their 2-hop topologies are not as similar as those of nodes G and H.

F   LIMITATIONS & BROADER IMPACTS

Broader Impacts. This paper presents work whose goal is to advance the field of Machine Learning. There are many potential societal consequences of our work, none which we feel must be specifically highlighted here.

Limitations. Our node IDs have proven to be effective in large-scale graphs by accelerating clustering and inference processes due to their low-dimensional nature. However, we have found that the number

of available datasets for very large networks is limited, and we acknowledge that there is still room for extension. Additionally, we believe that node IDs could benefit large language models, a topic we intend to explore more extensively in our future work.

G FURTHER RELATED WORKS

Vector Quantization (VQ). VQ compresses the representation space into a compact codebook of multiple codewords, using a single code to approximate each vector (Liu et al., 2024b). Advanced methods like VQ-VAE (Van Den Oord et al., 2017) and RQ-VAE (Lee et al., 2022) enhance quantization precision by employing multiple codebooks, initially for image generation and later adapted to recommender systems (Rajput et al., 2024; Liu et al., 2024c) and multimodal representation learning (Zheng et al., 2024; Xia et al., 2024). This paper introduces residual quantization for learning structure-aware node IDs, achieving superior feature compression performance.

Positional Encodings (PEs) as Graph Tokens. Transformer models with attention mechanisms can process graphs by tokenizing nodes and edges, incorporating positional or structural graph information through PEs (Müller et al., 2023). The Graph Transformer (Dwivedi & Bresson, 2020) and SAN (Kreuzer et al., 2021) initially employed Laplacian eigenvectors as PEs. Subsequent models like LSPE (Dwivedi et al., 2021) utilized random walk probabilities as node tokens. TokenGT (Kim et al., 2022) introduced orthogonal vectors for both node and edge tokens, and follow-up works also consider larger graphs (Luo et al., 2024c). However, these methods primarily encode the structural information of the graph and overlook the features of nodes, thereby constraining their direct application.